REVIEW

Check for updates

Expanding the horizons of covalent organic frameworks: sub-stoichiometric synthesis as an emerging toolkit for functional COFs

Samiyappan Vijayakumar, [ID] [ab] Ayyappanpillai Ajayaghosh [ID] *[ab] and Sreejith Shankar [ID] *[ab]

Covalent organic frameworks (COFs) are a class of porous materials generated from organic molecules resulting in two-dimensional (2D) or three-dimensional (3D) networks. Multifunctional molecules with defined symmetry react to give all-linked-COFs with pre-determined topologies. COFs and COF-based materials have continuously evolved *via* the exploration of new linkages, synthesis, and processing methodologies over nearly two decades. Several studies have contributed to the understanding of the formation mechanism and the influence of solvent(s), catalysts, and the reaction environment in the crystallization process. Apart from all-linked COFs with a "fully formed" network, sub-stoichiometric synthesis has been a recent development, where the change in stoichiometry of monomers results in generating unconventional topologies along with active functional groups within the pores of these materials. Thus, the generation and utilization of these "functional" COFs is an interesting challenge for reticular chemists, particularly in terms of the vast possibilities of applications that are not likely to emerge from conventional synthesis.

1. Introduction

The fundamental mechanistic understanding behind chemical transformations has evolved through a large realm of reagents, catalysis, and related synthetic strategies. The functionalization prospects of molecular materials have demonstrated the power of new synthetic methodologies in developing several intriguing chemical structures.[1,2] Though the possibilities for selectively functionalizing a particular position in the presence of many similar ones offer a toolbox for diversifying the properties and utility of a molecule, developing such a reliable methodology in terms of reagents, catalysts, and reaction conditions has been a challenging task.[3,4] The subtle differences in the intrinsic reactivity of similar functional groups in a molecule, under carefully controlled reaction conditions, could lead to site-selective and target-oriented syntheses, with a high degree of complementarity to conventional top-down and bottom-up approaches.[5,6] Site-selective approaches are indeed utilized by nature and envisage a better redox economy with improved synthetic modalities in natural product chemistry, drug discovery, and materials science.[7] Such strategies in biochemistry are aimed at understanding the mechanism behind biochemical processes, structure–activity relationship, and improved functions. For instance, non-covalent protection

strategies using nucleic acid aptamers have been demonstrated for the selective functionalization of molecules.[5]

With all the developments achieved in chemo- and stereo-selective syntheses over the past century, differentiating the reactivity among two or more reactive positions with identical or similar functional groups having negligible differences in their activation energy has been challenging.[4,8–10] Such a synthetic methodology is yet to be demonstrated to provide a general solution for the functional modification of complex molecular architectures in high yields and selectivity. While the use of protecting groups has been a preferred strategy for the selective reaction of similar functional groups in a molecule, the need for protection–deprotection steps hampers the efficiency of chemical reactions.[11–14] Therefore, modern synthetic chemistry advocates precise and selective recognition of minuscule differences in electronic and steric factors within potential reactive sites at the molecular level as the best approach towards achieving site-selective synthesis of complex chemical structures.[4,9,10] Identification of reaction conditions, including reagents, solvents, and catalysts, that complement the electronic, steric, and stereo-electronic attributes of the target functional group among several similar functional groups is critical for achieving archetypical site-selective transformations in synthetic chemistry.[8]

Achieving site selectivity among similar functional groups in polymerisation reactions is not fully explored with regard to the synthesis and utilization of functional polymeric systems. Reticular chemistry that utilizes the austerity and rigor of both organic and inorganic synthetic strategies has led to the

a Chemical Sciences and Technology Division, CSIR-NIIST, Thiruvananthapuram, 695 019, India. E-mail: ajayaghosh@niist.res.in; sreejith.shankar@niist.res.in

b Academy of Scientific and Innovative Research (AcSIR), Ghaziabad, 201002, India

development of a large number of extended porous crystalline solids, such as metal–organic frameworks (MOFs)[15–19] and covalent organic frameworks (COFs).[20–25] The dynamic but directional bond formation with microscopic reversibility in most of these materials has resulted in several intriguing properties emanating from highly functional complexities.[26–29] The structural matrices optimized through iso-reticular principles combined with the possibilities for post-synthetic modifications make these framework materials even more interesting.[30–33] The synthesis of complex structures of covalent organic frameworks (COFs) from organic molecular building units linked through covalent bonds, in this context, is a formidable task to achieve via functional group selective transformations. Nevertheless, unlike organic molecules, topology-driven selectivity towards chemically equivalent functional groups in reticular synthesis can be achieved by controlling the stoichiometry of the reactants.[34] While the dynamic covalent linkage stitches the atoms to the network backbone, unreacted functional groups decorate the pores, resulting in unprecedented properties and scope for post-synthetic modifications.[34–37] Therefore, in COFs, where organic building units are linked through covalent bonds, the choice of monomeric units allows for creating the desired network with unreacted functional groups, in line with site-selective synthesis in organic chemistry.

2. Selective transformations in COF synthesis

Reticular synthesis of COFs has shown wide applicability and has witnessed tremendous growth over the past couple of decades.[22,24,38] Connecting multifunctional molecules via preferentially dynamic covalent linkages to yield frameworks of various topologies has been accompanied by challenges related to crystallinity and structural elucidation.[39] Nevertheless, the synergistic efforts from synthetic chemists, theoreticians, and materials scientists have brought systematic advancements in this field.[40–43] Though we do not have a complete understanding of the formation of these networks, introduction of new synthetic approaches, crystallization methodologies, linkage chemistry, novel functional units, and processing strategies make this area an expanding and exciting field of research.[32,44–48]

Reaction of multifunctional monomers to give a fully formed network of COFs has been an ideal proposal for a long time.[41] The synthetic journey of COFs started with typically reversible linkages and later expanded to irreversible linkages and one-pot multicomponent reactions.[49–52] The field has also witnessed the utilization of unreacted sites, the introduction of non-interfering functional groups, and post-synthetic modifications that functionalize the pores or transform the linkages.[30,33,53] The functional versatility of such framework materials has led to various applications, including gas adsorption/separation,[54–57] host–guest chemistry,[58–61] sensing,[62–68] ion capture/transport,[69] catalysis,[70–76] and electrochemical applications.[77]

Focussed research activities on COFs that started with the first report via the formation of dynamic boroxine and boronate ester bonds have now been extended to seeded growth of 2D COFs, graphene nanoribbon 2D COFs, and recently to water harvesting frameworks.[78,79] One of the most investigated classes of COFs is imine-linked, which involves the reaction between aldehydes and amines.[80–83] Several synthetic approaches,[44,84–86] processing methodologies,[47,87,88] studies in terms of imparting structural stability[30,89–91] and mechanistic understanding of the formation under different conditions[81,85,92–97] have emerged over time. Post-synthetic introduction of primary amine groups or the presence of unreacted amino or carbonyl groups in imine-linked COFs have been shown to result in functional properties that are otherwise difficult to attain in fully formed networks.[98–101] In this context, several synthetic strategies, including functional group interconversions,[102–105] transamination reactions,[106,107] and site-selective[108–112] and regioselective synthesis,[113] have been reported to introduce primary amine groups in 2D COFs.

However, approaches like post-synthetic modification, transamination reactions, and site-selective and regioselective approaches are not devoid of limitations like complexity in the design of monomers, multiple steps, and challenges related to purification. These multistep synthetic approaches are still being utilized for incorporating active amine groups within imine-linked COFs.[114,115] While site-selective strategy is limited to selected orthogonally reactive monomers, the sub-stoichiometric approach allows for the facile synthesis of designed network materials solely based on their symmetry. The bottleneck in this approach is to identify the right solvent combination that facilitates the formation of crystalline networks with frustrated functional groups, which, however, is a challenge in conventional COF synthesis as well. Thus, the sub-stoichiometric approach is advantageous as compared to the existing methodologies for constructing functional COFs with active amine or aldehyde sites within imine-linked COFs. While the sub-stoichiometric synthesis of COFs is still in its infancy, several significant contributions demonstrating applications in various fields have emerged over the last five years. This article attempts to comprehensively review the current developments and provide future perspectives on the sub-stoichiometric synthesis of COFs and their applications. We believe that this article would support detailed investigations on sub-stoichiometric synthesis of 2D and 3D COFs, in order to advance further developments in this exciting area of research.

3. Sub-stoichiometric synthesis of 2D and 3D COFs

The last few years have witnessed the emergence of sub-stoichiometric synthesis capable of yielding either free amine or free aldehyde groups in imine-linked COFs (Fig. 1). This approach has not only resulted in unconventional topologies but also revived our understanding of mechanisms behind COF formation.

Though strategies like different solvent combinations and variations in stoichiometry of reactants were used, stoichiometry control gained significance with time, thereby giving rise to
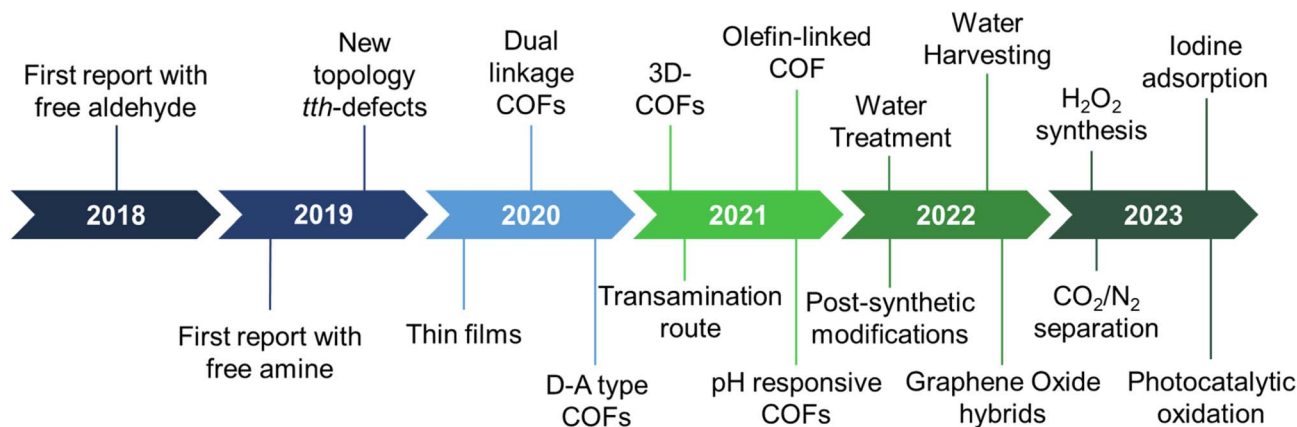
This journal is © The Royal Society of Chemistry 2023

J. Mater. Chem. A, 2023, **11**, 26340–26370 | **26341**

Fig. 1 Evolution of sub-stoichiometric synthesis of COFs and related reports.

the name sub-stoichiometric synthesis.[34,116] With the first report in 2018,[116] the sub-stoichiometric approach has so far yielded several 2D and 3D COFs *via* direct condensation of the monomeric units. Combined with functionalization prospects such as post-synthetic modification of frustrated groups, this approach has paved the way to utilize these networks in water harvesting, gas adsorption and separation, and extensively in photocatalysis. We anticipate this class of COFs, and the underlying synthetic challenges provide enough opportunities for reticular chemists to explore and comprehend. A brief timeline of the evolution of sub-stoichiometric approach in COF synthesis is given in Fig. 1.

While incomplete reactions may lead to unreacted functional groups, such COFs would possess low ordering and poor crystallinity, low stability, and non-uniform pore distributions within the network. Majority of the sub-stoichiometric (Type III) COFs are shown to be ordered, highly crystalline, stable, and possessing the expected porosity. The crystalline nature and ordering in sub-stoichiometric COFs are generally evident from XRD and porosity measurements. Theoretical calculation of the unit cell parameters further confirms the resulting structures. Moreover, the sub-stoichiometric approach generally yields unconventional topologies that are, in principle, not expected for all-linked COFs.[34] And the sub-stoichiometric structures obtained from tetratopic linkers are always presented with all-linked COFs. These observations are in favour of the "sub-stoichiometric" composition of monomers in Type III COFs as compared to incomplete reactions in all-linked COFs.

3.1 Evolution of new topologies and mixed linkages

While sub-stoichiometric approach provides a powerful tool to introduce either free aldehyde or amine groups in imine-linked COFs, the first three reports described the emergence of new topologies in 2D COFs.[34,116,117] Obtaining new topologies *via* sub-stoichiometric synthesis has aroused significant interest in terms of structure and applications of the resulting COFs, and subsequently, several groups have reported such COFs with multifarious applications.

The first report on sub-stoichiometric synthesis of COFs appeared in 2018 when Loh and co-workers utilized structurally

similar tetratopic aldehyde **1** and tetraphenylethylene (TPE) amine **2** to give fully condensed **TPE-COF-I** and partially condensed **TPE-COF-II** with frustrated carbonyls.[116] Variations in solvent and stoichiometry of the precursors **1** and **2** were found to result in two topologies. A 1 : 1 ratio of the aldehyde **1** and amine **2** in *o*-dichlorobenzene/*n*-butanol mixture yielded **TPE-COF-I** *via* a [4 + 4] condensation pathway, and a 2 : 1 ratio in 1,4-dioxane, *via* an unusual [2 + 4] pathway, yielded **TPE-COF-II** (Fig. 2). Since the influence of solvent(s), steric factors and nucleation mechanism was critical to the formation of the COFs, the approach was termed solvent-directed divergent synthesis. The unreacted linker units within the pores of **TPE-COF-II** were shown to have a significant impact on its CO_2 uptake capacity and a typically high value of 23.2 wt% (118.8 cm^3 g^{-1}) adsorption was observed at 1 atm and 273 K.

The term sub-stoichiometric synthesis was introduced in the very next year by Lotsch and co-workers and classified them as Type III COFs.[34] Tetratopic pyrene tetraaniline **3** upon condensation with tritopic triazine tribenzaldehyde **4** or benzene tripicolinaldehyde **5**, in an equimolar ratio in 1 : 1 mesitylene/dioxane under solvothermal conditions, yielded **PT-** and **PY-COFs** (Fig. 3). Sub-stoichiometric 2D COFs featuring imine linkages with an unexpected *bex* net topology and periodic unreacted amino groups were obtained from tri- and tetratopic linkers *via* a [4+3] mechanism. While fully formed networks and reasonable crystallinity cannot be expected from monomeric units with such symmetry, **PT-** and **PY-COFs** were obtained as crystalline solids. Contrary to the previous report from Loh and co-workers, variations in monomer feed ratio and solvent(s) did not yield distinctly different networks. In terms of functionalities, the free amino groups in **PT-** and **PY-COFs** led to better CO_2 sorption properties, post-synthetic modifications and organocatalytic performance. A tricomponent approach was further demonstrated to form *net*-like topologies using a ditopic linker leading to [4 + 3 + 2] COFs.

Concurrent with Lotsch's report on sub-stoichiometric synthesis,[34] Yaghi *et al.* published the synthesis of multinary COFs using hexa, tetra and trivalent linkers **6**, **9**, and **2** (Fig. 4).[117] Condensation reaction involving hexaminophenyl benzene **6**, tetrakis(4-aminophenyl) ethane **2**, and 1,3,5-tris(*p*-

26342 | *J. Mater. Chem. A*, 2023, **11**, 26340–26370
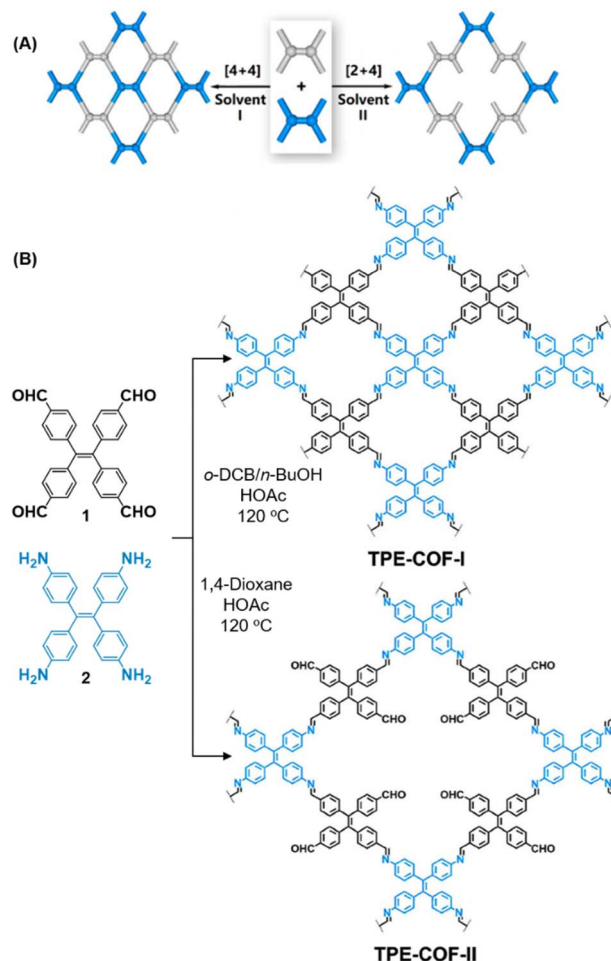
This journal is © The Royal Society of Chemistry 2023

Fig. 2 (A) Solvent-directed strategies used by Loh and co-workers for the construction of 2D-COFs with different topologies: fully formed network (**TPE-COF-I**, left) and partially formed frustrated-bonding structure (**TPE-COF-II**, right). (B) The corresponding synthetic scheme and the structures of the monomers (**1**, **2**) and the COFs. Reproduced from ref. 116 with permission from American Chemical Society, copyright 2018.
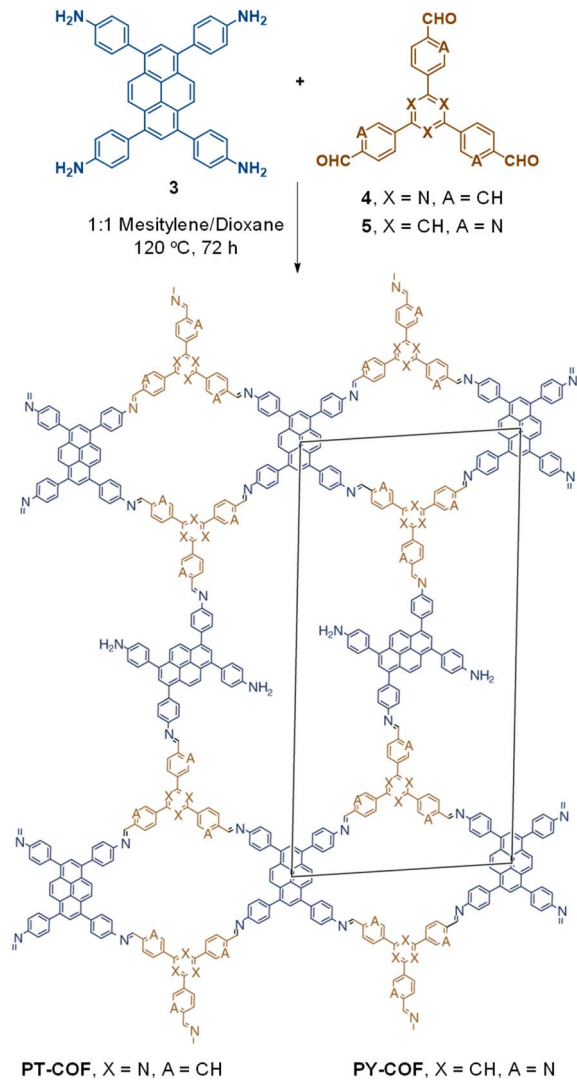

Fig. 3 Sub-stoichiometric synthesis of the imine linked **PT**- and **PY**-**COFs** from tetratopic pyrene tetraaniline **3** and triangular tritopic triazine tribenzaldehyde **4** or benzene tripicolinaldehyde **5**. Reproduced from ref. 34 with permission from Springer Nature, copyright 2019.

formylphenyl)benzene **8** resulted in a complex network of **COF-346** with unprecedented *tth* topology. In addition, crystalline, porous **COF-360** with a rare *kgd* topology and **COF-340** with a defective *tth* topology were also reported in the same study. However, variations in the ratio of the monomers were not found to afford COFs with different structural attributes or topologies.

The sub-stoichiometric approach has also allowed the construction of 1D COFs with residual functionalities, which could further be converted to 2D COFs with mixed linkages. A year after the reports on **COF-340**, **COF-346** and **COF-360**, Yaghi and co-workers constructed 1D ribbons of **COF-76** with unreacted amino groups from 1,3,6,8-tetrakis(*p*-formylphenyl) pyrene **10** and tris(4-aminophenyl)amine **11**. The free amines in these 1D ribbons were subsequently interlinked using aldehyde or anhydride to yield 2D frameworks of imine linked **COF-77** or imide linked **COF-78**, respectively (Fig. 5).[35] The 1D **COF-76** was prepared *via* modulator (*p*-toluidine) assisted synthesis using C$_3$

symmetric monomers **10** and **11** in a 1 : 2 sub-stoichiometric ratio, catalysed by trifluoroacetic acid. The structural stability and porosity of the 1D ribbons facilitated the crosslinking reaction involving free amino groups to yield the corresponding 2D networks. A one-pot synthesis for the construction of **COF-77** and two step one-pot synthesis for the construction of **COF-78** were also reported. This work further demonstrates the use of sub-stoichiometric synthesis for the construction of COFs with dual linkages.

3.2 Sub-stoichiometric synthesis of 3D COFs

Extension of the sub-stoichiometric approach to construct 3D COFs was first demonstrated in 2021 by Peng and co-workers.[118] During an attempt to construct a network of *she*/*nts* or *het* topologies, a frustrated 3D network with unreacted carbonyls
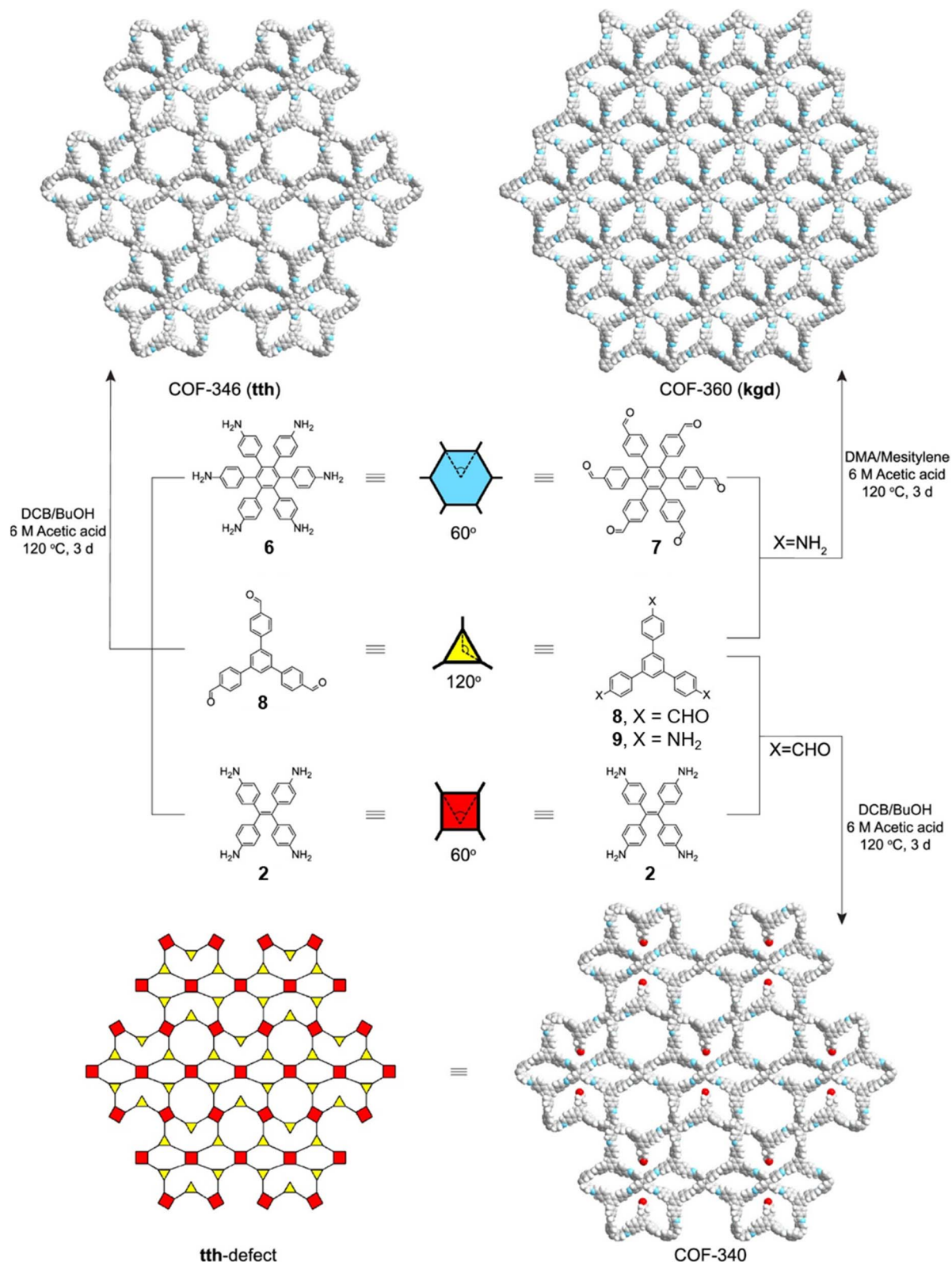
This journal is © The Royal Society of Chemistry 2023

J. Mater. Chem. A, 2023, **11**, 26340–26370 | **26343**

Fig. 4   Synthetic scheme for **COF-346**, **COF-360** and **COF-340**. The structures of the corresponding monomeric units are also shown along with the topologies of the COFs. Reproduced from ref. 117 with permission from American Chemical Society, copyright 2019.

was obtained. A 2D COF (**2D sql COF**) was also synthesized *via* the partial condensation of hexaldehyde phenyl benzene **7** and a tetramine derivative of tetraphenylethylene **2** (Fig. 6A and B).

However, use of 3,3′,5,5′-tetra(*p*-aminophenyl)-bimesitylene **12** as the amino counterpart resulted in a 3D COF (**3D pts COF**) with *pts* topology (Fig. 6A and C).
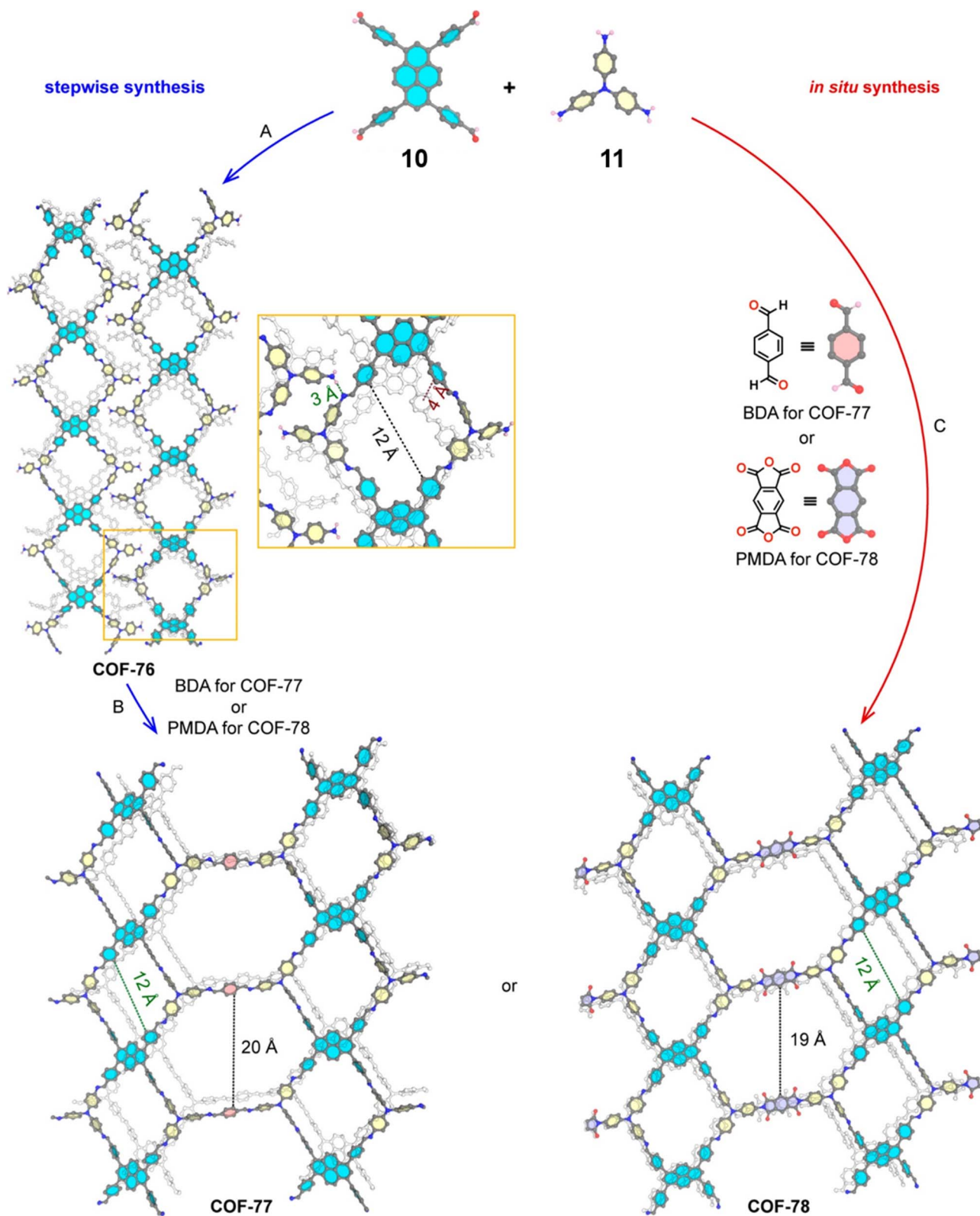
Fig. 5 Scheme for the sub-stoichiometric imine linked 1D **COF-76** with residual amines from the tetra-aldehyde **10** and tri-amine **11** in a 1 : 2 stoichiometric ratio and further conversion into 2D **COF-77** and **COF-78** using aldehyde and anhydride monomers *via* stepwise (A and B) and *in situ* methods (C). Reproduced from ref. 35 with permission from American Chemical Society, copyright 2020.
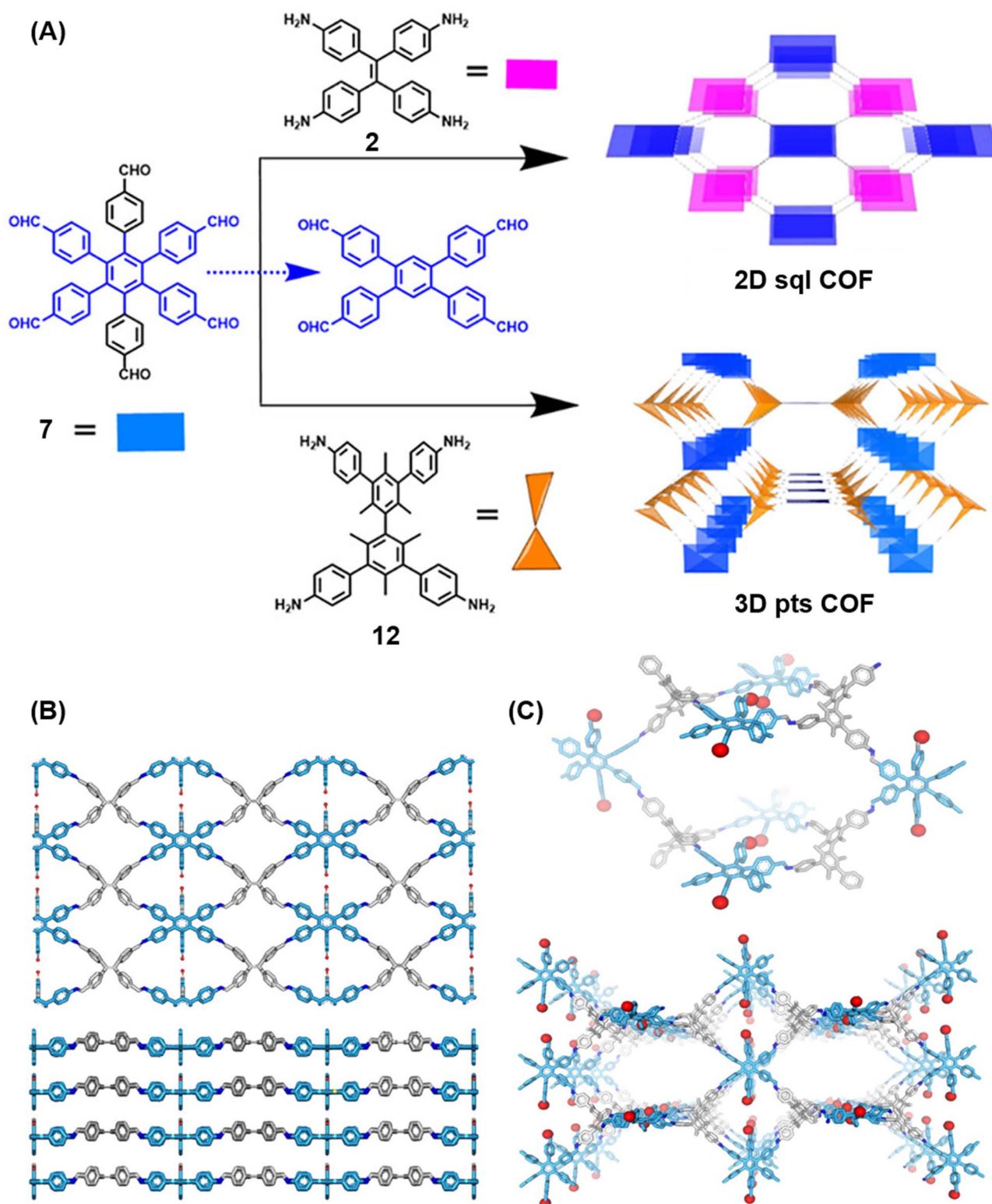
This journal is © The Royal Society of Chemistry 2023

J. Mater. Chem. A, 2023, **11**, 26340–26370 | **26345**

Fig. 6 (A) Sub-stoichiometric synthesis of COFs with *sql* and *pts* topologies from the monomeric units **7**, **2**, and **12**. (B) Top and side views of the ball-and-stick structural model for **2D sql COF**. **7** is shown in blue, **2** is shown in grey, and O atoms are shown in red. (C) Cage type architecture and the ball-and-stick structural model for **3D pts COF**. **7** is shown in blue, **12** is shown in grey, and O atoms are shown in red. Reproduced from ref. 118 with permission from American Chemical Society, copyright 2021.

3D pts COF characterized by a surface area of 3478 m² g⁻¹, which is among the highest reported for 3D imine-linked COFs.[118] The high surface area as well as the presence of unreacted aldehyde groups in the COFs further resulted in excellent gas storage properties. Both **2D sql COF** and **3D pts COF** exhibited preferential gas adsorption properties in the

26346 | *J. Mater. Chem. A*, 2023, **11**, 26340–26370

This journal is © The Royal Society of Chemistry 2023

order C_2H_2 > CO_2 > CH_4 at ambient conditions. Though **3D pts COF** was found to possess a higher surface area compared to **2D sql COF**, the adsorption capacities of the former were found be inferior to those of the latter. It is proposed that the higher adsorption of C_2H_2 over CO_2 was most likely due to the polarizability and quadruple moment of the gases, which interact with residual carbonyls in pores. Theoretical modelling corroborated that hydrogen bonding between the acetylene hydrogen and the residual carbonyls is the reason behind high adsorption capacities of the COFs.

Creating a long-range microporous order in framework materials has been an interesting field of investigation over the past decade.[119–127] Yue and co-workers have reported the synthesis of amine functionalised 3D COFs **COF-300-0914** and **COF-300-1114** *via* a non-stoichiometric synthon (NSS) strategy by varying the ratio of tetrakis(4-anilyl) methane **13** and terephthaldehyde **14** (Fig. 7).[36] Adjusting the ratio of the monomers **13** : **14** to 11 : 14 in a solvothermal condensation procedure led to **COF-300-1114** with unreacted amino groups which allowed the pores to be impregnated with a larger amount of Pd(II) salts, that upon hydrogenation resulted in Pd nanoparticle decoration of the pores, while retaining the structure of the parent COF (Fig. 7). The presence of Pd NPs was confirmed through energy dispersive X-ray spectroscopy and ICP-MS techniques, resulting in a mass loading of 1–2%, while more than 90% of the Pd content was confirmed to be Pd(0) by XPS. While both **COF-300-0914** and **COF-300-1114** confined ultra-small Pd nanoclusters within their pores, the presence of more unreacted amino groups in the latter restricted NP aggregation *via* Pd–N coordination. These Pd-decorated COFs were further used as catalysts for benzyl alcohol oxidation reactions with up to 97% conversion with 99% selectivity.

3.3 Applications of COFs constructed *via* sub-stoichiometric synthesis

Robust morphology, high surface area, large pore volume, and high thermal and chemical stabilities make COFs suitable candidates for several applications including gas storage/separation, catalysis, energy storage, *etc.*[23,38,128,129] While the formation of ideal crystals of framework materials is challenging, the defects or unreacted sites in such materials open up new avenues that are otherwise difficult to explore.[98,99,130–132] Nevertheless, the introduction of free amine and carbonyl groups with periodic order is generally difficult to achieve in conventional COFs with an imine linkage. Therefore, several reports on the sub-stoichiometric synthesis of COFs are aimed at constructing network materials with a rational arrangement of either of the functional groups, for expanding their applications. This section of the article attempts to review the applications of COFs obtained *via* sub-stoichiometric approaches.

3.3.1 Adsorption. In general, imine-linked COFs constructed through sub-stoichiometric synthesis are characterized by the presence of either free aldehyde or amine groups.[34,36,133,134] These heteroatomic functionalities are capable of having electrostatic interactions with gaseous
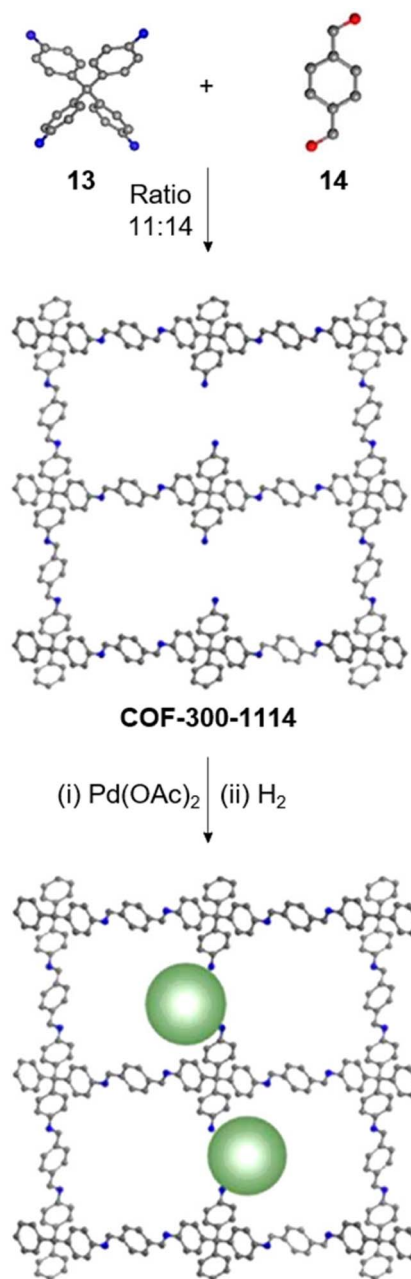

Fig. 7 Non-stoichiometric synthesis of **COF-300-1114** from the amine **13** and aldehyde **14** followed by Pd impregnation and subsequent reduction yielding the Pd/COF composite. Color code: grey, carbon; blue, nitrogen; red, oxygen. H-atoms are omitted for clarity. Reproduced from ref. 36 with permission from American Chemical Society, copyright 2020.

molecules.[118,134] Incorporation of amino or carbonyl groups has been a preferred strategy towards enhancing CO_2 uptake in porous materials, particularly under humid conditions.[107,135–140] Polar functional groups in pores are also capable of forming non-covalent interactions, especially hydrogen bonds with water molecules and provide the opportunity to detect or store moisture.[78,79,141–147] For instance, the first reported sub-stoichiometric COF with free carbonyl groups has been
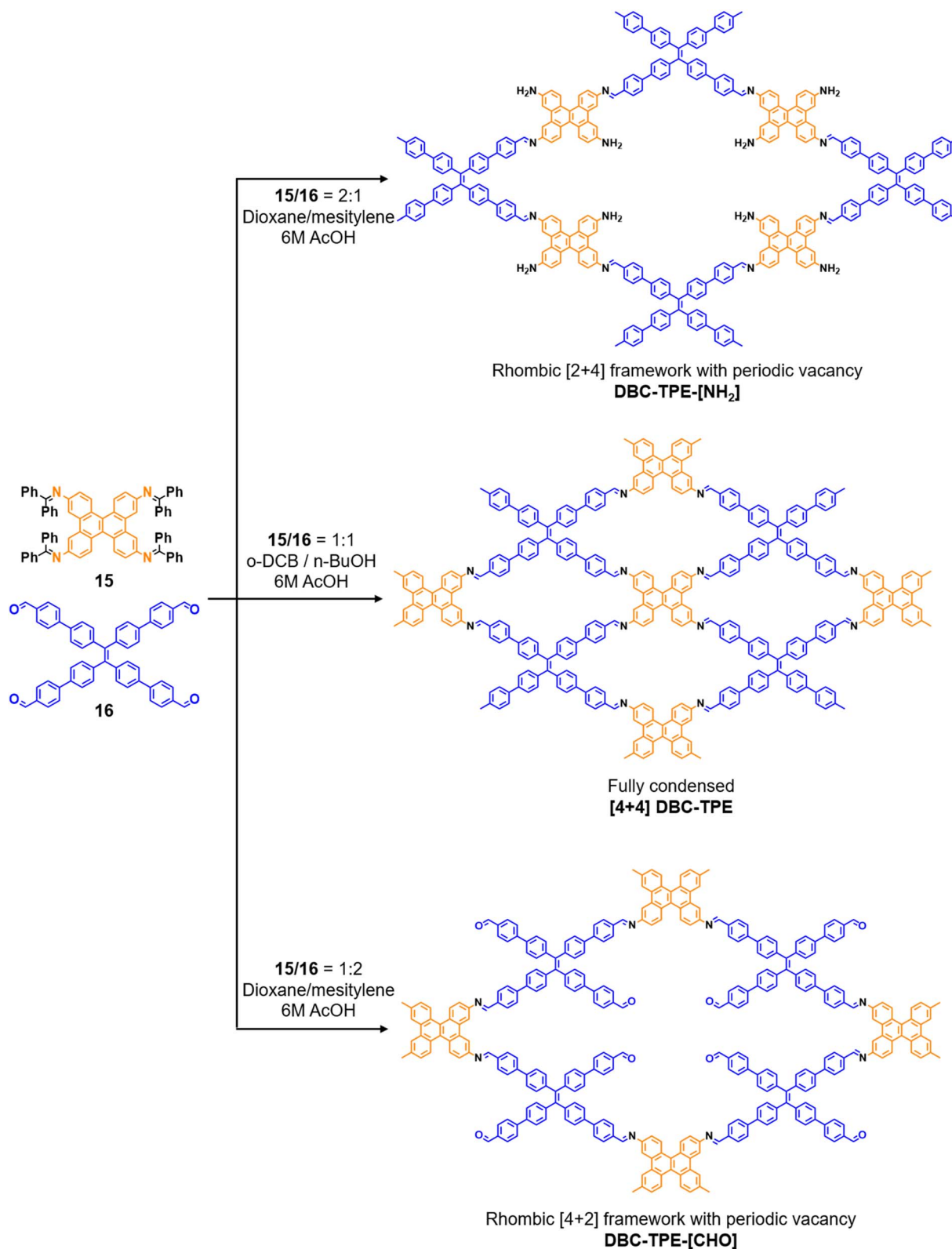
This journal is © The Royal Society of Chemistry 2023

J. Mater. Chem. A, 2023, **11**, 26340–26370 | **26347**

Fig. 8 Sub-stoichiometric synthesis of imine linked 2D COFs **DBC-TPE-[CHO]**, **DBC-TPE** and **DBC-TPE-[NH₂]** with residual aldehydes and amines from the same monomers *via* a transamination approach.

demonstrated for CO_2 capture.[116] As mentioned previously, at 1 atm pressure, **TPE-COF-II** (Fig. 2B) showed a CO_2 adsorption of 23.2 wt% (118.8 cm³ g⁻¹) and 11.8 wt% (60.5 cm³ g⁻¹) at 273 and

298 K, respectively. Similarly, Lotsch *et al.* have reported that **PT-COF** and **PY-COF** (Fig. 3) at 1 atm and 273 K exhibited CO_2 uptake values of 95 mg g⁻¹ and 146 mg g⁻¹, respectively. These

26348 | *J. Mater. Chem. A*, 2023, **11**, 26340–26370

This journal is © The Royal Society of Chemistry 2023

adsorption capacities are ~1.5 times higher than those of similar COFs without free amino groups.[34]

Chen and co-workers have demonstrated a transamination approach to construct COFs with frustrated aldehyde and amino groups.[138] This was the first instance of constructing a COF with free amine and aldehyde functionalities using a sub-stoichiometric approach from the same monomeric units by simple alteration in their ratios. Different molar ratios (1 : 2, 1 : 1 and 2 : 1) of dibenzo[g,p]chrysene **15** and tetraphenylethene tetraldehyde derivative **16** were used to construct three COFs, **DBC-TPE-[CHO]**, **DBC-TPE** and **DBC-TPE-[NH₂]**, respectively (Fig. 8). Surface area exceeding 1000 m² g⁻¹ and thermal stability above 400 °C were observed for all three COFs. **DBC-TPE-[NH₂]** with free amino groups exhibited the highest CO_2 uptake of 3.16 mmol g⁻¹, followed by **DBC-TPE-[CHO]** with free aldehyde groups (2.56 mmol g⁻¹) and the fully formed network **DBC-TPE** (2.39 mmol g⁻¹) at 273 K. The free functionalities in these COFs were also shown to adsorb water, most likely due to hydrogen bonding. Volumetric water vapor sorption experiments at 298 K revealed water uptake capacities of 0.42 g g⁻¹, 0.40 g g⁻¹, and 0.26 g g⁻¹ for **DBC-TPE-[NH₂]**, **DBC-TPE** and **DBCTPE-[CHO]**, respectively. The relatively higher water adsorption properties of **DBC-TPE-[NH₂]** are attributed to the lowering of the inflexion point due to the presence of hydrophilic amines, suggesting better water adsorption properties under less humid conditions.

Ma and co-workers have recently reported COFs with residual carbonyls for selective adsorption of CO_2.[134] Three COFs, **HFPB-Stb-D**, **HFPB-TAPB-D**, and **HFPB-ETTA-D**, were constructed via sub-stoichiometric reactions involving C₆-symmetric aldehyde monomers (hexa(4-formylphenyl)-benzene **7**) and amine monomers of various symmetry (C₂ – 4,4′-diaminostilbene **17**; C₃ – 1,3,5-tris(4-aminophenyl) benzene **9**; and C₄ – tetrakis(4-aminophenyl)ethene **2**, Fig. 9A). This work tendered, for the first time, monomer symmetry regulated directional defects for *in situ* functionalization of COFs with a periodic distribution of aldehyde groups for selective interactions with CO_2. Better structural stability, availability of aldehyde groups and good crystallinity of **HFPB-Stb-D**, **HFPB-TAPB-D**, and **HFPB-ETTA-D** resulted in high CO_2 uptake values of 128.9 cm³ g⁻¹ (25.3 wt%), 109.6 cm³ g⁻¹ (21.5 wt%) and 44.9 cm³ g⁻¹ (8.8 wt%), respectively at 1 bar pressure and 273 K. Their CO_2 adsorption capacities at low pressure (0.1 bar) and at 298 K were also seen to follow the same order. The CO_2 adsorption capacity of the defective COFs was found to depend preferentially on the number of homogeneously distributed aldehyde groups in the framework as compared to other factors such as specific surface area, pore volume, or nitrogen content. In fact, **HFPB-Stb-D** exhibited one of the best reported selective separation values (45.8 from Ideal Adsorbed Solution Theory (IAST)) for CO_2/N_2 among other COFs. This differential adsorption of gases is due to the reasonably lower quadrupole moment of N_2 compared to residual aldehydes as validated by theoretical calculations (Fig. 9B).

An emissive donor–acceptor type **COF-SMU-1** having frustrated aldehyde groups, with a quantum yield of 6.8%, has
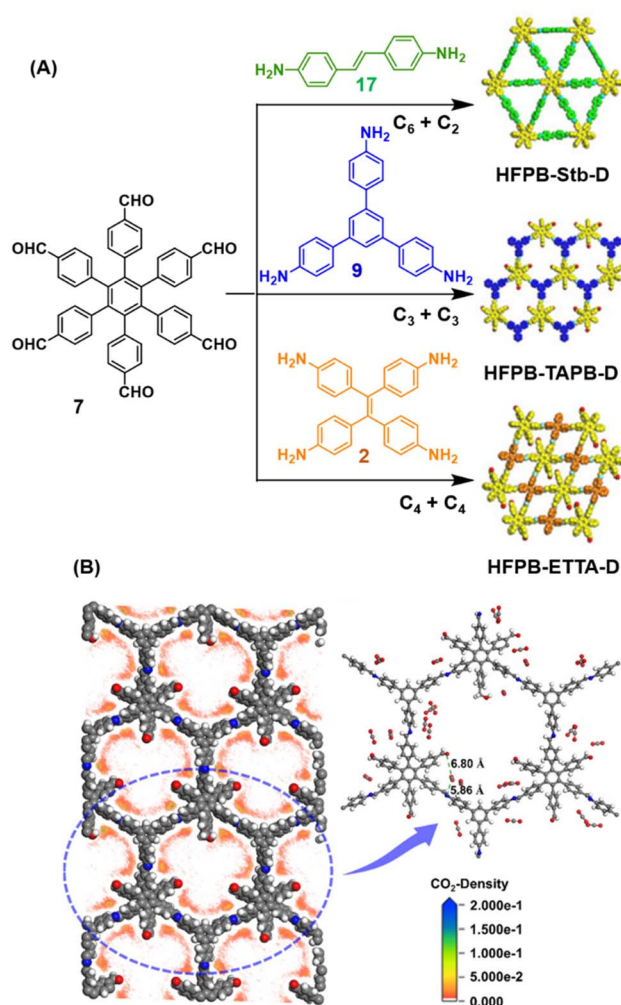

Fig. 9 (A) Synthesis of the COFs **HFPB-Stb-D**, **HFPB-TAPB-D**, and **HFPB-ETTA-D** from the C₆-symmetric aldehyde monomer (hexa(4-formylphenyl)-benzene **7**) and amine monomers of various symmetry (C₂ – 4,4′-diaminostilbene **17**; C₃ – 1,3,5-tris(4-aminophenyl) benzene **9**; and C₄ – tetrakis(4-aminophenyl)ethene **2**). (B) CO_2 distribution density in **HFPB-TAPB-D** (left) and the simplified stick model (right), where H, C, N, and O are marked in white, grey, blue, and red, respectively. Reproduced from ref. 134 with permission from American Chemical Society, copyright 2023.

recently been reported via sub-stoichiometric synthesis involving a triamine **18** and a tetra-aldehyde **10** by Das and co-workers (Fig. 10A).[148] **COF-SMU-1** exhibited solvatochromic properties due to polarity dependent π–π interactions of pyrene units present in the neighbouring layers. The color of **COF-SMU-1** was found to undergo a rapid change from yellow to reddish brown when exposed to water vapour (Fig. 10B). **COF-SMU-1** when dispersed in acetonitrile, showed a slight bathochromic shift and a gradual decrease in emission intensity upon addition of water (3.6% v/v). Water that hydrogen bonds with triazine, imine and aldehyde impacts the D–A charge transfer (Fig. 10B, right). This interaction of water with residual carbonyls was established via spectroscopic techniques and a water-uptake value as high as 14.0 mmol g⁻¹ (0.25 g g⁻¹) was observed for **COF-SMU-1** at

This journal is © The Royal Society of Chemistry 2023

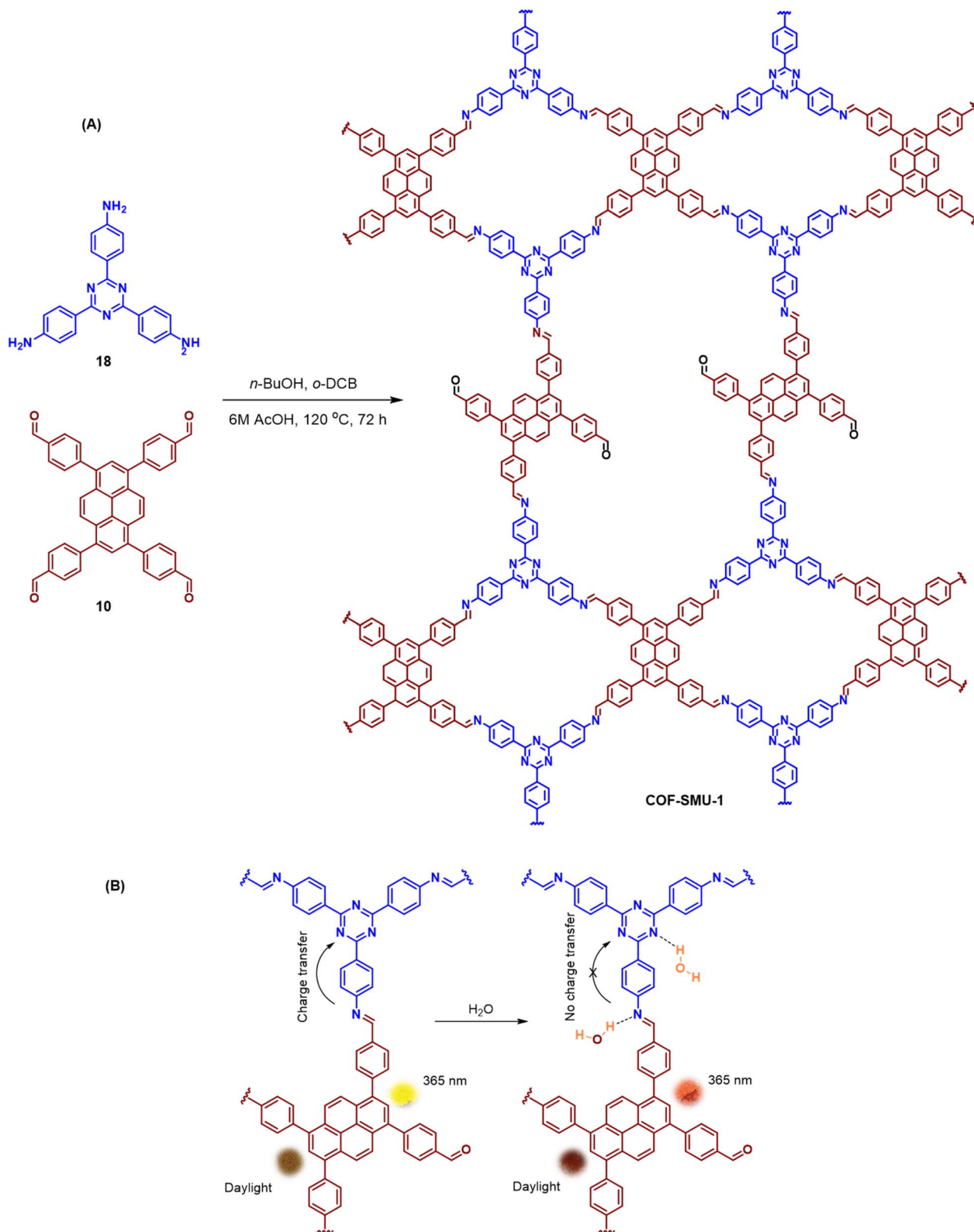J. Mater. Chem. A, 2023, **11**, 26340–26370 | **26349**

Fig. 10 (A) Sub-stoichiometric synthesis of the COF **COF-SMU-1** from a triamine **18** and a tetra-aldehyde **10** based monomeric unit. The unreacted aldehyde sites are shown in green. (B) Repeating units and water sensing mechanism of **COF-SMU-1**. Adapted from ref. 148 with permission from Wiley, copyright 2023.
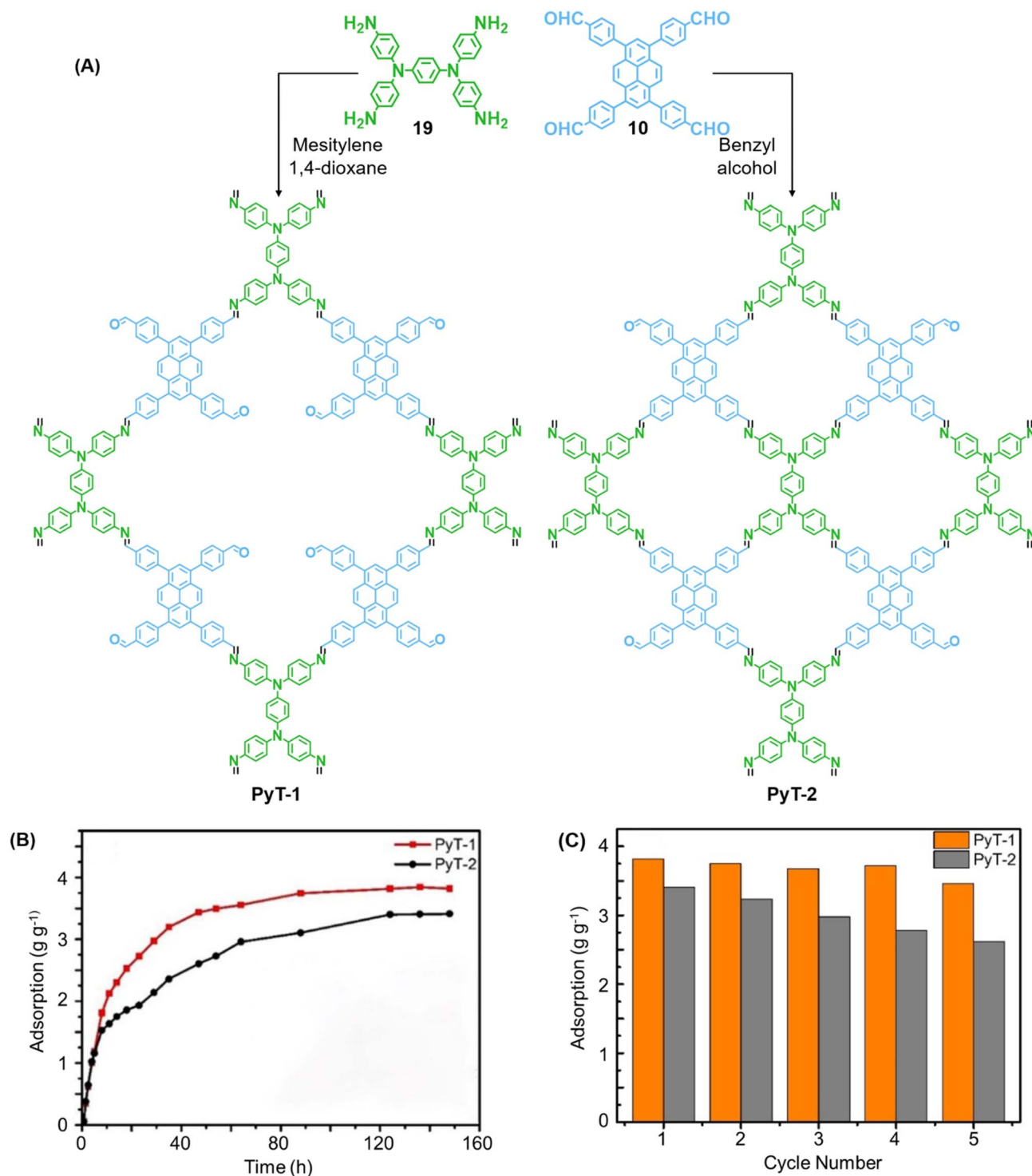
26350 | *J. Mater. Chem. A*, 2023, **11**, 26340–26370

This journal is © The Royal Society of Chemistry 2023

Fig. 11 (A) Synthesis of the COFs PyT-1 and PyT-2 from tetratopic monomers 19 and 10. (B) Iodine vapor adsorption capacities of PyT-1 and PyT-2 at 75 °C and atmospheric pressure and (C) the corresponding cycling performance. Reproduced from ref. 149 with permission from MPDI, copyright 2023.

25 °C. Even in the presence of hydrophobic aromatic polycycles, high water adsorption properties are correlated to the abundance of imine and carbonyl groups in the COF structure. The absence of a significant reduction in porosity for prolonged exposure to moisture suggests that COF-SMU-1 may have application as a potential water harvester.

In 2023, Tian and co-workers reported the synthesis of $[C_4 + C_4]$ COF PyT-2 and $[C_4 + C_2]$ COF PyT-1 from tetrabenzaldehyde 19 and tetraamine 10 via the variation in the choice of solvents alone (Fig. 11A).[149] While both the COFs exhibited good thermal, solvent, acid–base stabilities, PyT-1 was found to have comparably higher BET surface area (1186.94 m^2 g^{-1}) and pore

This journal is © The Royal Society of Chemistry 2023

J. Mater. Chem. A, 2023, **11**, 26340–26370 | **26351**

volume (0.89 cm^3 g^{-1}). Significant iodine vapour adsorption was observed for both **PyT-1** and **PyT-2** for the first 10 h and attained saturation around 90 h (>3.4 g g^{-1}, Fig. 11B). Desorption was effected by rinsing the COFs in ethanol. **PyT-1** was found to retain an adsorption efficiency >90% after five adsorption–desorption cycles, while **PyT-2** showed a lower efficiency of 75–76% (Fig. 11C). Solution phase adsorption studies were conducted using *n*-hexane solutions of iodine and both COFs were found to follow pseudo second order kinetics.

3.3.2 Catalysis

3.3.2.1 Heterogeneous organocatalysis. Lotsch and co-workers, while introducing the term 'sub-stoichiometric synthesis' in COFs, further demonstrated free amines in **PT-** and **PY-COFs** (Fig. 3) capable of catalysing room temperature synthesis of substituted chromenes.[34] The aromatic amines in the frameworks were found to catalyse the regioselective cyclization–substitution cascade reactions of 2-hydroxylcinnamaldehyde with trimethylsilyl enol ether, with yields of 22% and 8%, respectively, for **PT-** and **PY-COFs**. The proposed catalytic cycle begins with a Schiff base adduct formed between the residual amines and 2-hydroxylcinnamaldehyde. As previously mentioned, the Pd-decorated **COF-300-0914** and **COF-300-1114** (Fig. 7), reported by Yue *et al.*,[36] were also used as catalysts for benzyl alcohol oxidation reactions with excellent yield and selectivity.

In 2020, Xie and co-workers demonstrated the first instance of using type III COFs as photocatalysts. Three D–A type COFs

TTCOFs 1-3 were synthesized from C$_2$ symmetric tetraphenyl-ethylene based monomers **1**, **5**, and **2**, and C$_3$ symmetric triazine-based monomers **4** and **17**, under acidic conditions over 5–9 days (Fig. 12A).[150] While **TTCOFs 1** and **2** featured a *bex* topology with optical bandgaps >2 eV, **TTCOF-3** was characterized by a *tth* topology with a lower band gap of 1.73 eV. These COFs were used as photocatalysts in visible light driven selective α-functionalization of tertiary amines. **TTCOF-2** was found to provide the best results in direct aerobic cross-dehydrogenative coupling between 2-phenyl-1,2,3,4-tetrahydroisoquinoline **19** and nitromethane or ketones *via* a radical mechanism (Fig. 12B). Furthermore, the same COF was also found to be active in photoconversion of aryl boronic acids into the corresponding phenols.

3.3.2.2 Photocatalysis. While the photoconversion of aryl boronic acids into the corresponding phenols catalysed by **TTCOF-2** was reported by Xie and co-workers in 2020,[150] the extension of the sub-stoichiometric approach to the synthesis of olefin linked COFs was first demonstrated by Cai and co-workers in 2021.[151] **PTO-COF** with a *bex* net topology was synthesized through sub-stoichiometric Knoevenagel condensation of 1,3,6,8-tetrakis(*p*-formylphenyl)-pyrene **10** and 2,4,6-trimethyl-1,3,5-triazine **22**. The mechanochemical synthesis of β-keto enamine linked COF **TpMaCOF** from triformylphloroglucinol **23** and melamine **24** was integrated with the mechanochemical delamination of bulk **PTO-COF** to construct a heterojunction. Subsequently, 2D/2D **TpMa/PTO-COFs**
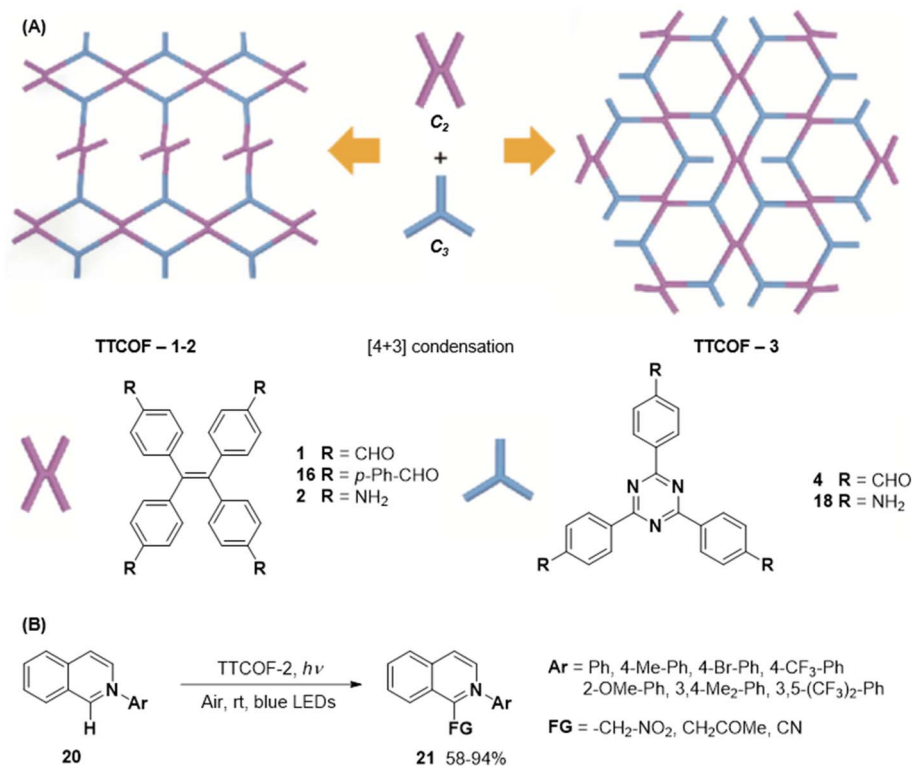

Fig. 12 (A) Schematic representation of the synthesis of **TTCOFs–1-3** from C$_2$ symmetric tetraphenylethylene based monomers **1**, **16**, and **2**, and C$_3$ symmetric triazine-based monomers **4** and **18**. (B) Photocatalyzed aerobic cross-dehydrogenative coupling between 2-phenyl-1,2,3,4-tetrahydroisoquinoline **20** and nitromethane or ketones. Reproduced from ref. 150 with permission from Science China Press, copyright 2020.
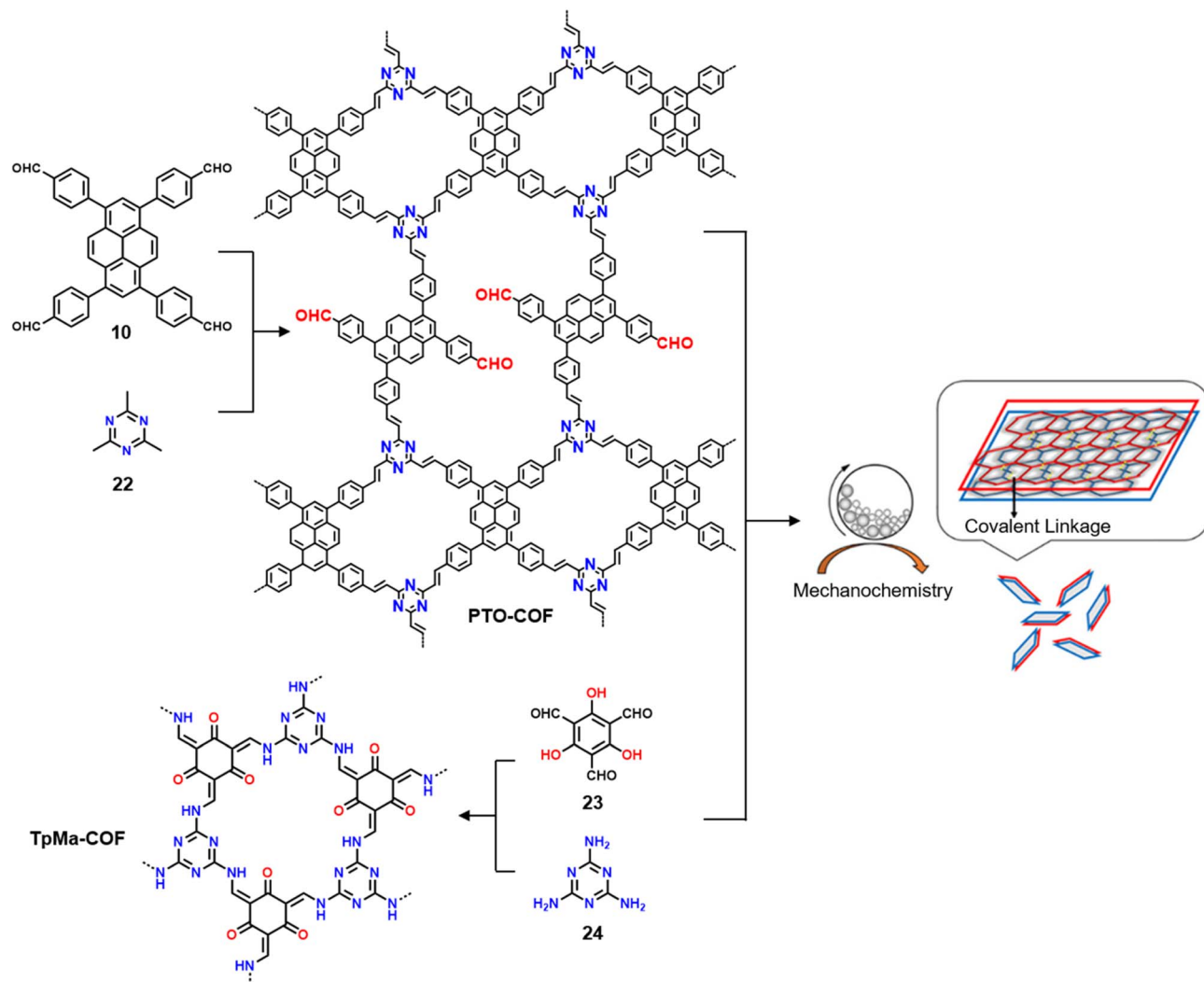
26352 | *J. Mater. Chem. A*, 2023, **11**, 26340–26370

This journal is © The Royal Society of Chemistry 2023

Fig. 13 Schematic representation of the synthesis of the **PTO-COF** (from monomers **10** and **22**), **TpMa-COF** (from monomers **23** and **24**), and the 2D/2D **TpMa/PTO COF** heterojunctions. Reproduced from ref. 151 with permission from American Chemical Society, copyright 2021.

heterojunctions were constructed by one-pot ball milling of the monomers **23** and **24** and **PTO-COF** in different ratios, *viz* **TpMa : PTO** = 1 : 2, 1 : 1, 2 : 1, and 3 : 1 (Fig. 13) with bandgaps of ~2.5 eV. These heterojunctions exhibited high photocurrents and electron transfer efficiency with a small interfacial resistance compared to the individual parent COFs. Photocatalytic performance of these materials towards the degradation of sulfamethazine, an antibiotic model, under the irradiation of visible light ($\lambda > 420$ nm) was further evaluated. The 2D/2D COF with a **TpMa : PTO** ratio of 2 : 1 was found to show a high degradation rate of 98.4% within 50 min of light irradiation. The rate constant of degradation (1.04×10^{-3} s^{-1}) was indeed more than twice that of **PTO-COF** and approximately double that of **TpMa-COF**. The intense photocurrent response coupled with small charge transfer impedance is most likely the reason behind the better photocatalytic properties of the heterojunction, and the photocatalytic degradation was found to originate from the photogenerated holes and the superoxide radicals.

A year later, Lan and co-workers reported the substoichiometric synthesis of imine-linked **TCOF** and **ECOF** with a *bex* net topology from tri- and tetra-topic linkers **25**, **16**, and **18**.[37] Addition of the amine functionalized polyoxometalate (POM) cluster of MnMo$_6$–2NH$_2$ resulted in its covalent attachment with uncondensed aldehydes in the pores of these COFs (Fig. 14A–C). Incorporation of POM within the pores was confirmed by FT-IR, XPS, elemental mapping, transmission electron microscopy and NMR. The amount of the POM in **TCOF**-MnMo$_6$ was found to be 25.9 wt%.

The COF with its inherent light absorption combined with the catalytic properties of CO$_2$ adsorbing POM crystals was proposed as an effective catalyst for the photoreduction of CO$_2$ to CO. Reaction in a gas–solid reactor with CO$_2$ and water vapour yielded more than two times conversion for **TCOF**-MnMo$_6$ (796.6 μmol g^{-1}) compared to **ECOF**-MnMo$_6$ (365.3 μmol g^{-1}) and exceeded that for previously reported POM- and COF-based CO$_2$ photoreduction catalysis. The photocatalytic activity of individual COFs, POM alone or a physical mixture of
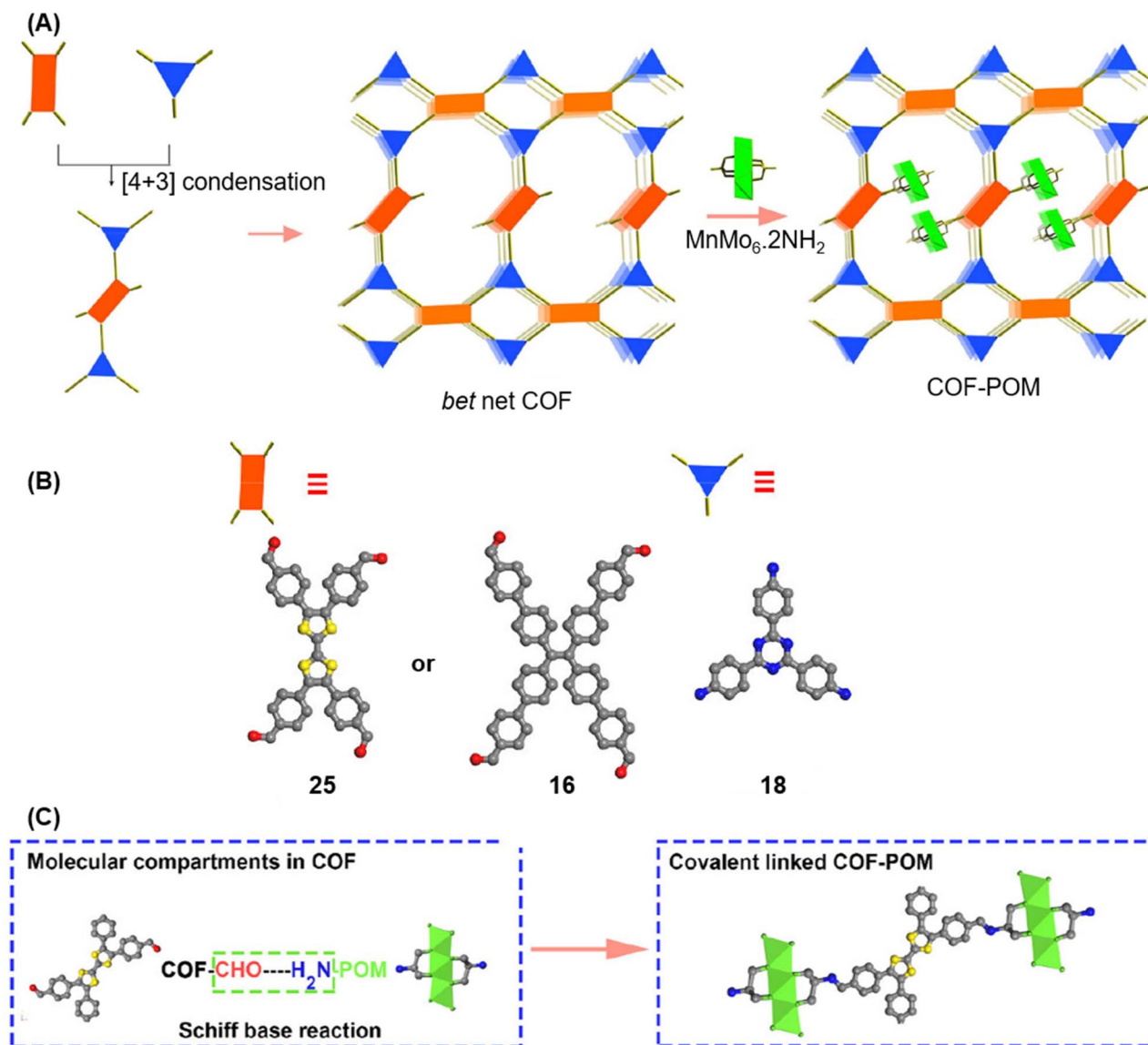
Fig. 14 (A) Schematic representation of the synthesis of **TCOF** and **ECOF** and uniformly dispersed POM clusters within their pores *via* covalent linkages. (B) Ball and stick model of the monomers **25**, **16**, and **18**. (C) Schematic representation of the molecular compartments in the COFs formed *via* Schiff Base reaction (left) and the formation of covalently linked COF–POM hybrids (right). Color code: grey, carbon; blue, nitrogen; red, oxygen. H-atoms are omitted for clarity. Reproduced from ref. 37 with permission from American Chemical Society, copyright 2022.

both the materials was found to be rather low compared to the hybrid, which in turn confirmed the functional significance of incorporating a POM with a COF through a covalent linkage.

Gu and co-workers have recently reported a COF **Bpy-TAPT** with dual active sites and polar aldehyde groups, comprising of triazine and bipyridine units, from a tetratopic linker **26** and the tritopic linker **18**, *via* a substoichiometric approach (Fig. 15A).[133] While other derivatives and analogues were also synthesized, a high photocatalytic generation of H_2O_2 from water (4038 µmol h^{-1} g^{-1}) was observed for **Bpy-TAPT**. This rate of H_2O_2 generation in the absence of any sacrificial reagents and stabilizers was significantly higher compared to prior reports on COF-based photocatalysts (Fig. 15B). Theoretical calculations

confirmed that the HOMO and LUMO of **Bpy-TAPT** were partly localized on the bipyridine and triazine units, suggesting them to be the oxidative and reductive sites, respectively. The dual active sites were found to improve the visible-light-response and enhanced charge generation, while the free aldehyde groups allowed for effective separation of carriers and adsorption of O_2/H^+ on the surface of **Bpy-TAPT**.

Hu and coworkers have reported two COFs **TPE-TPB-A** (Type-I) and **TPE-TPB-B** (Type-III) just by varying the solvent composition (*n*-butanol/mesitylene or *n*-butanol/dioxane), using a 1 : 1 molar ratio of the amine **2** and the aldehyde **27** in the presence of 6 M acetic acid for 5 days at 120 °C (Fig. 16A).[152] Both the COFs exhibited high surface area
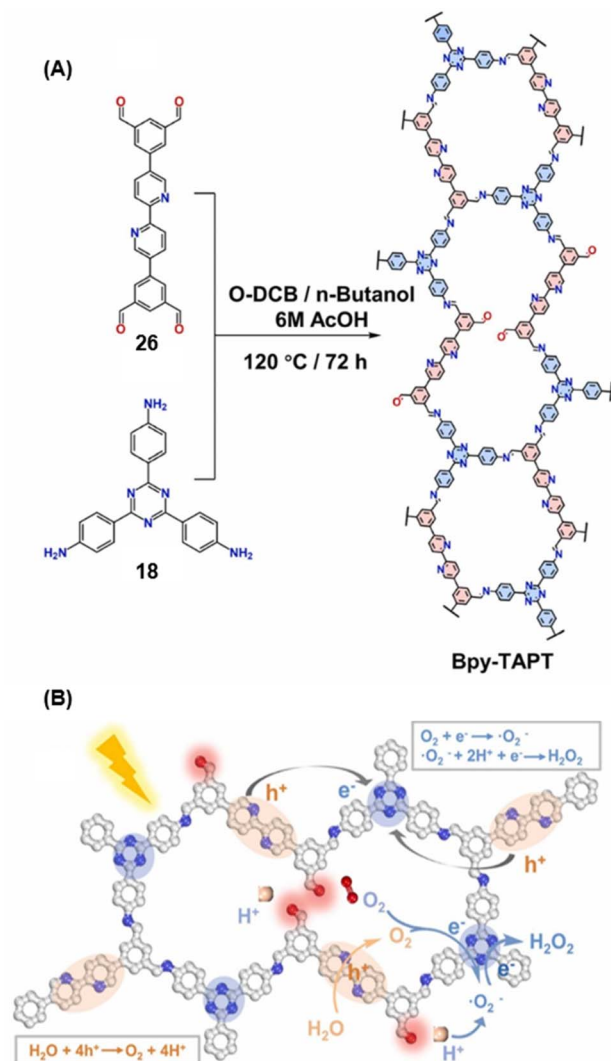
26354 | *J. Mater. Chem. A*, 2023, **11**, 26340–26370

This journal is © The Royal Society of Chemistry 2023

Fig. 15 (A) Sub-stoichiometric synthesis of the COF **Bpy-TAPT** from the monomers **26** and **18**, showing the presence of unreacted aldehyde sites. (B) Photocatalytic generation of H_2O_2 from water using **Bpy-TAPT** and its postulated mechanism. Reproduced from ref. 133 with permission from Elsevier, copyright 2023.

Fig. 16 (A) Synthesis of the COFs **TPE-TPB-A** (type-I) and **TPE-TPB-B** (type-III) from the monomers **2** and **27**. Unreacted aldehyde sites are shown in **TPE-TPB-B**. (B and C) Comparison of the photocatalytic hydrogen generation capabilities of **TPE-TPB-A** and **TPE-TPB-B**. Reproduced from ref. 152 with permission from American Chemical Society, copyright 2023.

($\sim$1000 m^2 g^{-1}), with similar water adsorption characteristics ($\sim$450 cm^3 g^{-1} at P/P_o = 0.98). The stepwise water adsorption characteristics and comparably low water contact angle (78.9°) of **TPE-TPB-B** signifies the role of dangling formyl groups in making the pores hydrophilic. Experimental observations and theoretical calculations related to the energy and active sites for water adsorption confirmed that **TPE-TPB-B** is more hydrophilic than **TPE-TPB-A** due to the presence of carbonyl groups. The photocatalytic hydrogen evolution (PHE) from both the COFs was analysed using a platinum cocatalyst and ascorbic acid as a sacrificial agent. Irradiating **TPE-TPB-A** and **TPE-TPB-B** with visible light (>420 nm, 6 h) resulted in hydrogen generation at a rate of 43.53 and 510.2 μmol h^{-1} g^{-1}, respectively (Fig. 16B). Both the COFs exhibited reasonably high photostability under continuous irradiation for 24 h.
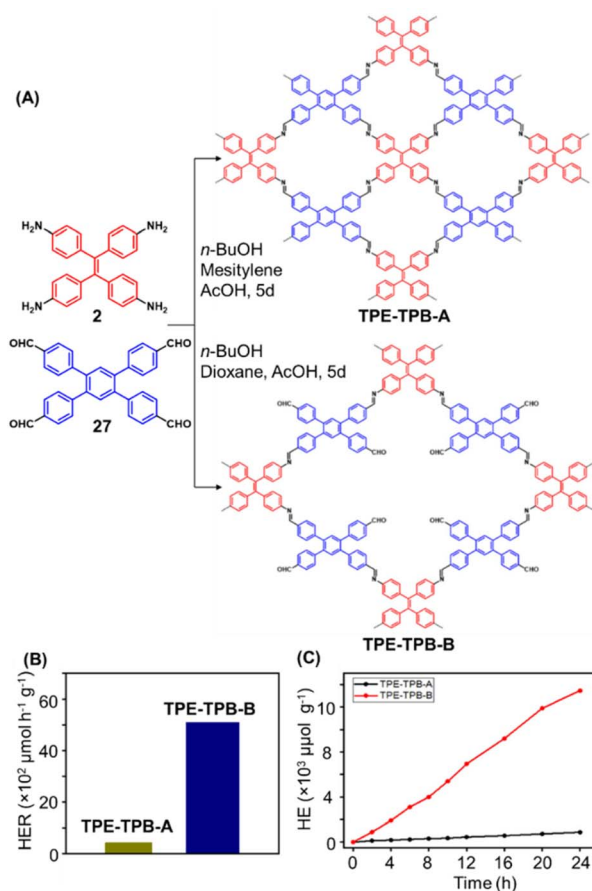
TPE-TPB-B displayed almost 15.3 times higher PHE rate than **TPE-TPB-A** (Fig. 16C), mediated by efficient electron transfer from the COF to the platinum cocatalyst.

Qiu and co-workers have reported a sub-stoichiometric photoresponsive COF **TAPP-TFPT** using a porphyrin derivative **28** and the triazine trialdehyde **4** as monomers.[153] Silver nanoparticles were then deposited over the COF *via* a post-synthetic modification to obtain the composite material Ag@**TAPP-TFPT** for the photocatalytic conversion of toxic bis(2-chloroethyl) sulfide (CEES) to non-toxic bis(2-chloroethyl) sulfoxide (Fig. 17A). The parent COF **TAPP-TFPT** and the composite Ag@**TAPP-TFPT** were evaluated for the degradation of CEES. While the oxidation of CEES was found to be complete within 15 min ($t_{1/2}$ = 6.5 min), when using Ag@ **TAPP-TFPT** as a photocatalyst, **TAPP-TFPT** took 25 min for the reaction ($t_{1/2}$ = 10.5 min, Fig. 17B).

The catalytic efficiency was found to be two-fold higher under an oxygen atmosphere than in ambient air (Fig. 17C), with 98% conversion retained after five cycles. The strong surface plasmon resonance of silver nanoparticles along with
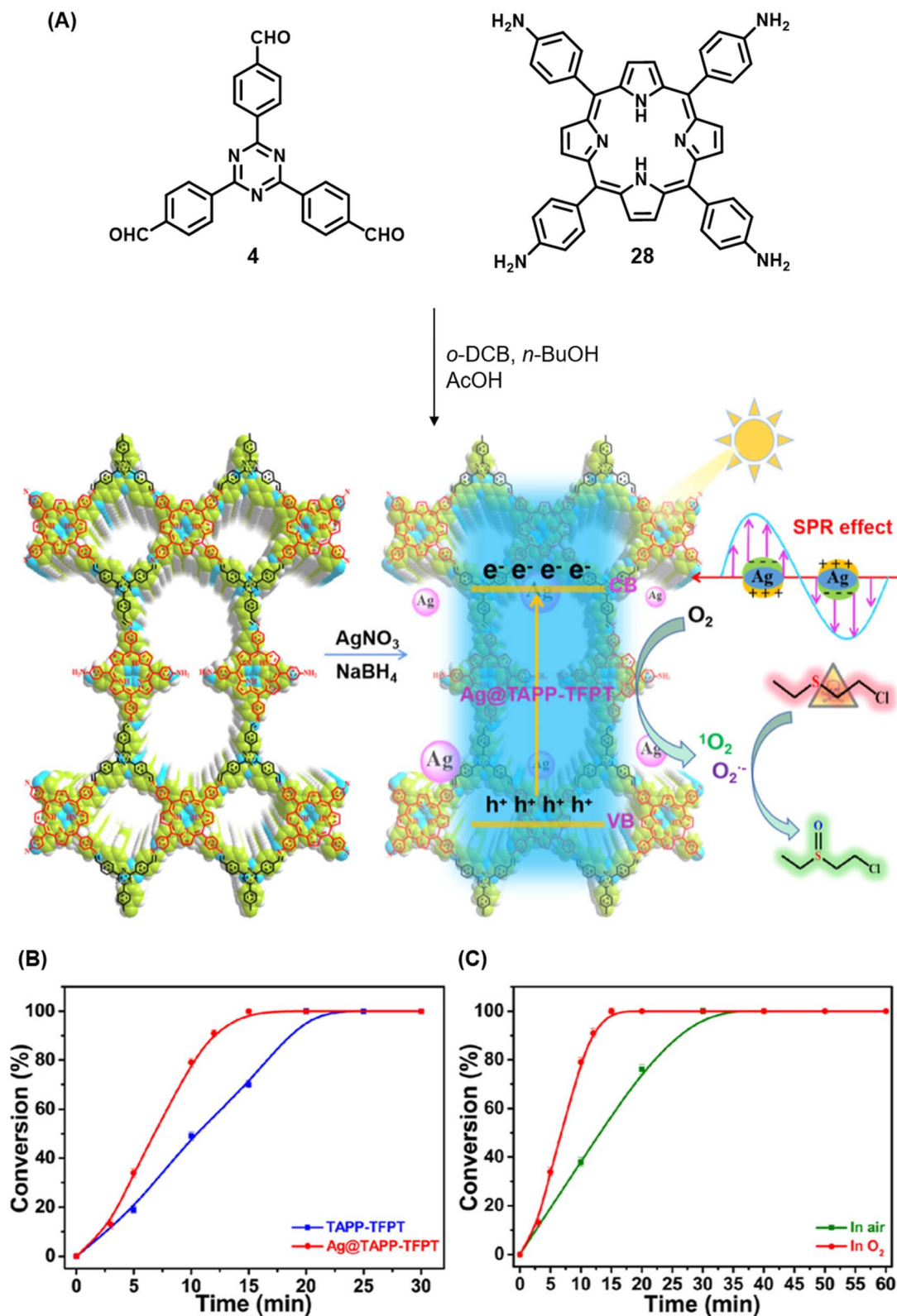
This journal is © The Royal Society of Chemistry 2023

J. Mater. Chem. A, 2023, **11**, 26340–26370 | **26355**

Fig. 17 (A) Synthesis of the COFs **TAPP-TFPT** and **Ag@TAPP-TFPT** from the monomers **4** and **28**. Silver nanoparticles were deposited over **TAPP-TFPT** *via* a post-synthetic modification to obtain **Ag@TAPP-TFPT**. (B) Comparison of the photocatalytic efficiency of **TAPP-TFPT** and **Ag@TAPP-TFPT** in converting bis(2-chloroethyl) sulphide (CEES) to bis(2-chloroethyl) sulfoxide. (C) Comparison of the catalytic efficiency under ambient air and oxygen. Reproduced from ref. 153 with permission from American Chemical Society, copyright 2023.

26356 | *J. Mater. Chem. A*, 2023, **11**, 26340–26370

This journal is © The Royal Society of Chemistry 2023

efficient electron–hole separation in Ag@**TAPP-TFPT** resulted in increased absorption in the visible region with a concomitant decrease in the band gap, thereby fostering enhanced photocatalytic activity. EPR measurements confirmed that both $^1O_2$ and $O_2^{\cdot-}$ were involved in the oxidation process.

3.3.3 Pollutant removal. A large number of as-synthesized and membrane-immobilized COFs have shown wide applications in micropollutant removal, oil water separation, decontamination of metal ions and biological applications.[154–162] Carbon allotropes containing COF hybrids are also known to improve their physicochemical properties for energy and environmental applications.[163–165] In this context, the first report on a hybrid material comprising of a COF synthesized *via* a sub-stoichiometric approach (**TT-COF**) and graphene oxide (GO) appeared in 2022.[166] **TT-COF** with built-in formyl groups were constructed using a C_2 symmetric tetraphenylethylene tetraldehyde **16** and C_3 symmetric amino triazine **9** (Fig. 18).

The hybrid material N6-GO@**TT-COF**-*x* (*x* = amount of COF, 0–8 mg) was prepared by spreading **TT-COF** over dispersed GO on a Nylon-66 substrate. Exposed formyl groups were found to facilitate the dispersion of the COF on GO, and large area defect-free continuous layers were fabricated *via* hot pressing. Owing to the presence of active sites and vertical channels stacked by regular pores, **TT-COF** exhibited a large flux of 309.99 L m^{-2} h^{-1} bar^{-1} and high rejection of 99.5% for cationic dyes with molecular weight above 500 Da. The membrane was unaffected by acidic or basic conditions and could be reused for many cycles without any detectable loss in crystallinity or activity.

3.3.4 Energy storage. COFs and their hybrids, with redox active sites, high surface area and structural stability at different pH and temperature, are widely used in energy storage applications. An *in situ* topological deformation strategy to construct a weakly ordered sub-stoichiometric COF in the presence of GO was demonstrated for the first time by Xi and co-workers.[167] Two GO containing COFs, **D-[4+3]COFs 1 and 2**, were synthesized *in situ* from the triamine derivative of triazine **18** and the tetraaldehydes **1** and **16**, respectively (Fig. 19A). Since the presence of GO induced the rearrangement of COF nanosheets while hindering interlayer stacking, this strategy benefited from enhancing the size, count and accessibility of pores as well as exposure of active sites and polar groups for shorter mass transport pathways and better redox activity. The induced stacking disorder directly reflected in the weakened plane reflections in XRD when compared to the native COFs prepared in the absence of GO. Uniform distribution of sulphur within **D-[4+3]COFs** was achieved *via* better channel accessibility due to weakened stacking along with the presence of exposed polar carbonyl groups (Fig. 19B and C). These hybrid COFs were used as sulphur cathode carriers of Li–S batteries with high loading, effective anchoring of polysulfides and reduced the Li$^+$ transport distance, leading to better electrochemical performance (Fig. 19D). With high storage capacities up to 1057 mA h g^{-1} at 0.5C and >85% retention after 500 cycles, these COFs outperform similar systems reported in the literature. The
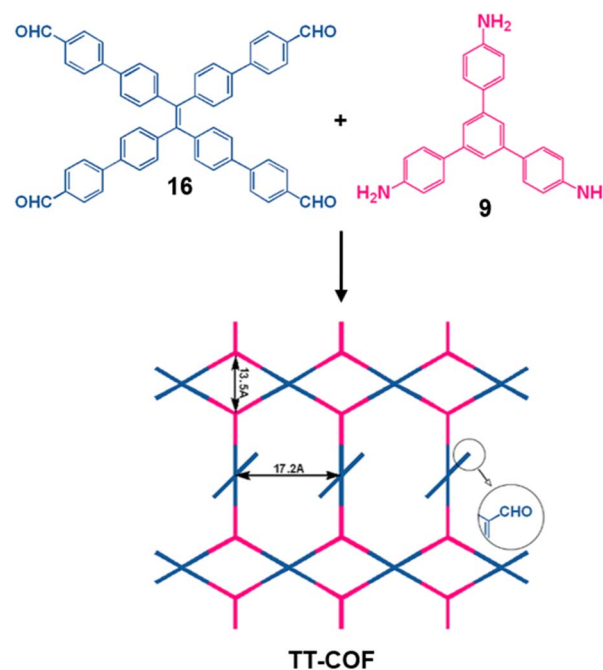

Fig. 18 Sub-stoichiometric synthesis of the TT-COF from the monomers **16** and **9**, showing the presence of unreacted aldehyde sites. Reproduced from ref. 166 with permission from Elsevier, copyright 2022.

localization of significant positive charges on the benzene rings due to the presence of an electronegative imine bond and the formyl groups, as shown in the electrostatic potential images, most likely contribute to the superior electrochemical performance of **D-[4+3]COFs** based electrodes.

3.3.5 Photodetectors. Lu and co-workers in 2020 reported photosensitive donor–acceptor sub-stoichiometric 2D-COF–graphene heterostructures using the monomers **18** and **16** (Fig. 20A).[168] Well-defined 2D heterostructures of **COF$_{ETBC–TAPT}$** were grown on a single-layer graphene and the corresponding photodetector device was set up using Au electrodes on a Si/SiO$_2$ substrate (Fig. 20B).

A clean thin film structure of **COF$_{ETBC–TAPT}$** was confirmed by scanning electron microscopy (Fig. 20C). The **COF$_{ETBC–TAPT}$**–graphene heterostructure was characterized by a p-type architecture and a photocurrent of 1.79 μA was observed under a low illumination power of 0.67 μW cm^{-2}. A photoresponsivity as high as 3.2×10^7 A W^{-1} for a light power of 0.1 pW (3.3 nW cm^{-2}), with an external quantum efficiency of 8.5×10^9% and a fast response time of 1.14 ms, with cycling stabilities exceeding 800 on–off cycles, was observed for the COF hybrid. Furthermore, polar molecules like ammonia and ethanol were found to chemically interact with the free aldehyde groups in the pores of **COF$_{ETBC–TAPT}$** and had a corresponding impact on the photoelectric performance of the device, with a sensitivity of 16.2% and 5.8% for 1% NH$_3$ and 1% ethanol vapour in air, respectively.

3.3.6 pH response. Chen and co-workers have reported two COFs, **TPE-Por-2** and **TPE-Por-4**, from the porphyrin-based amines **29 and 30** and aldehyde **1** (Fig. 21).[169] The selectivity

This journal is © The Royal Society of Chemistry 2023

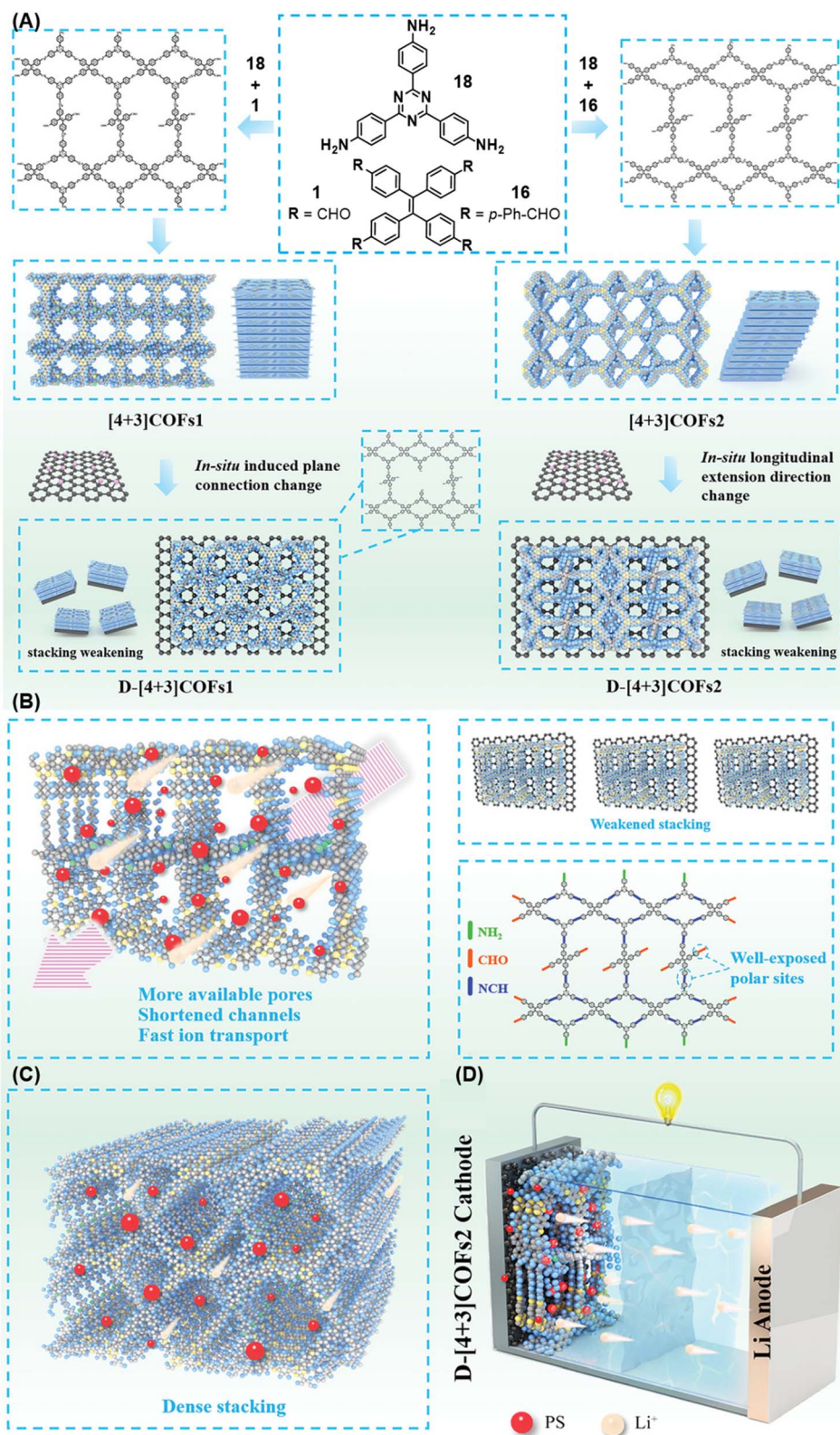*J. Mater. Chem. A*, 2023, **11**, 26340–26370 | **26357**

Fig. 19 Schematic representation of (A) the sub-stoichiometric synthesis of [4+3] and D-[4+3] COFs and the topology deformation of D-[4+3] COFs *via* the introduction of graphene oxide during synthesis, the (B) reduced and (C) dense stacking in [4+3] and D-[4+3] COFs, respectively, and (D) the Li–S battery assembled with D-[4+3] COFs. Reproduced from ref. 167 with permission from Wiley, copyright 2023.
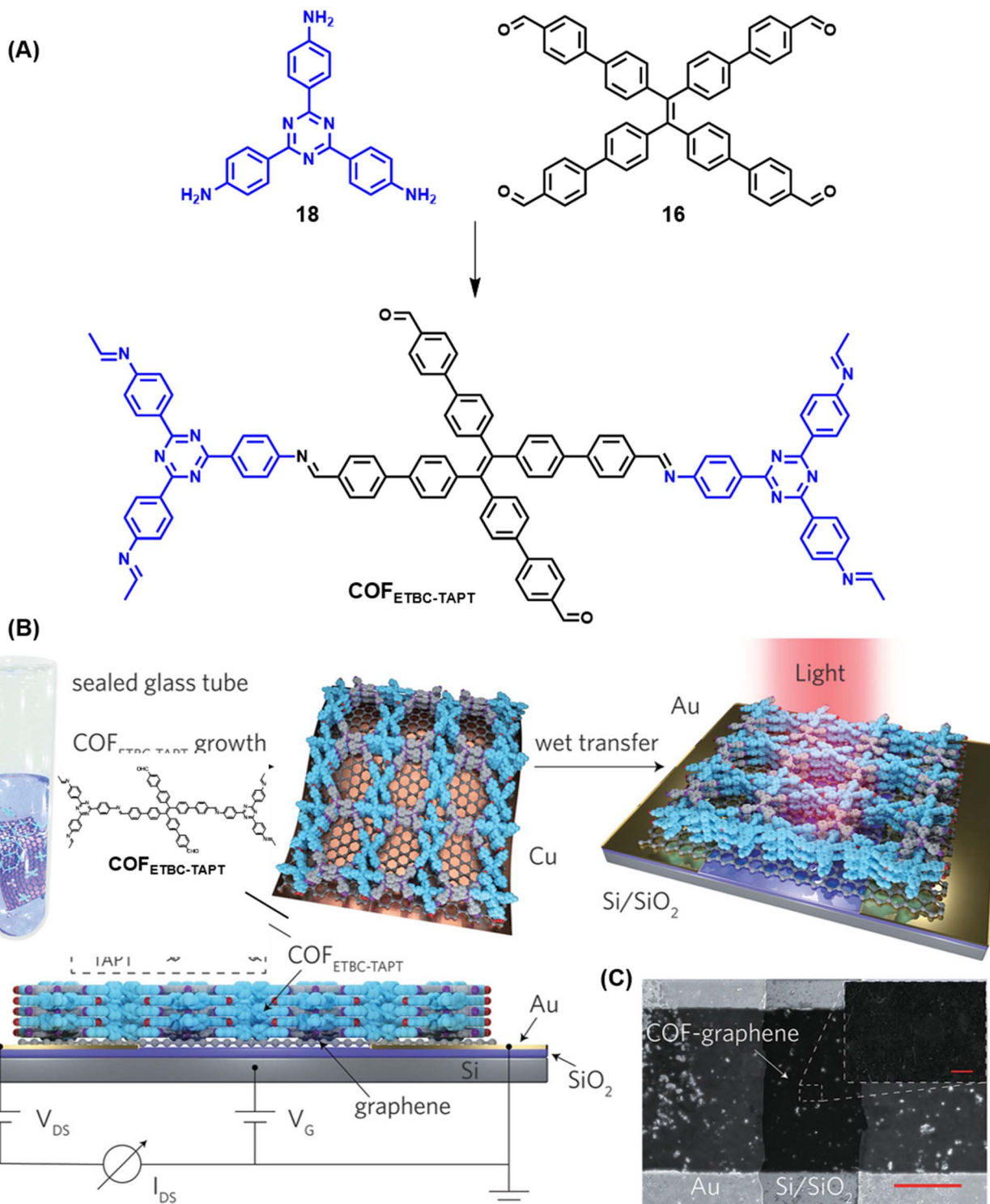
26358 | *J. Mater. Chem. A*, 2023, **11**, 26340–26370

This journal is © The Royal Society of Chemistry 2023

Fig. 20 Schematic representations of (A) the sub-stoichiometric synthesis of $COF_{ETBC-TAPT}$ from the monomers **18** and **16**, and (B) oriented growth of $COF_{ETBC-TAPT}$ on Cu-supported graphene and its wet transfer on to Au electrodes on a Si/SiO$_2$ substrate (top) and the side view of the photodetector set-up (bottom). (C) The SEM images of the photodetector constructed using $COF_{ETBC-TAPT}$ (scale bar = 20 μm) and the corresponding enlarged image (scale bar = 1 μm). Reproduced from ref. 168 with permission from Wiley, copyright 2020.

in the formation of formyl group tethered **TPE-Por-4** is justified by the effect of the solution phase self-assembly process, pore selection and steric hindrance. Both the COFs were emissive due to the presence of the tetraphenylethylene core. Irradiating the THF dispersion of the COFs (λ_{max} = 430 nm) resulted in emissions at 672 nm and 686 nm for **TPE-Por-2** and **TPE-Por-4**,

This journal is © The Royal Society of Chemistry 2023

J. Mater. Chem. A, 2023, **11**, 26340–26370 | **26359**
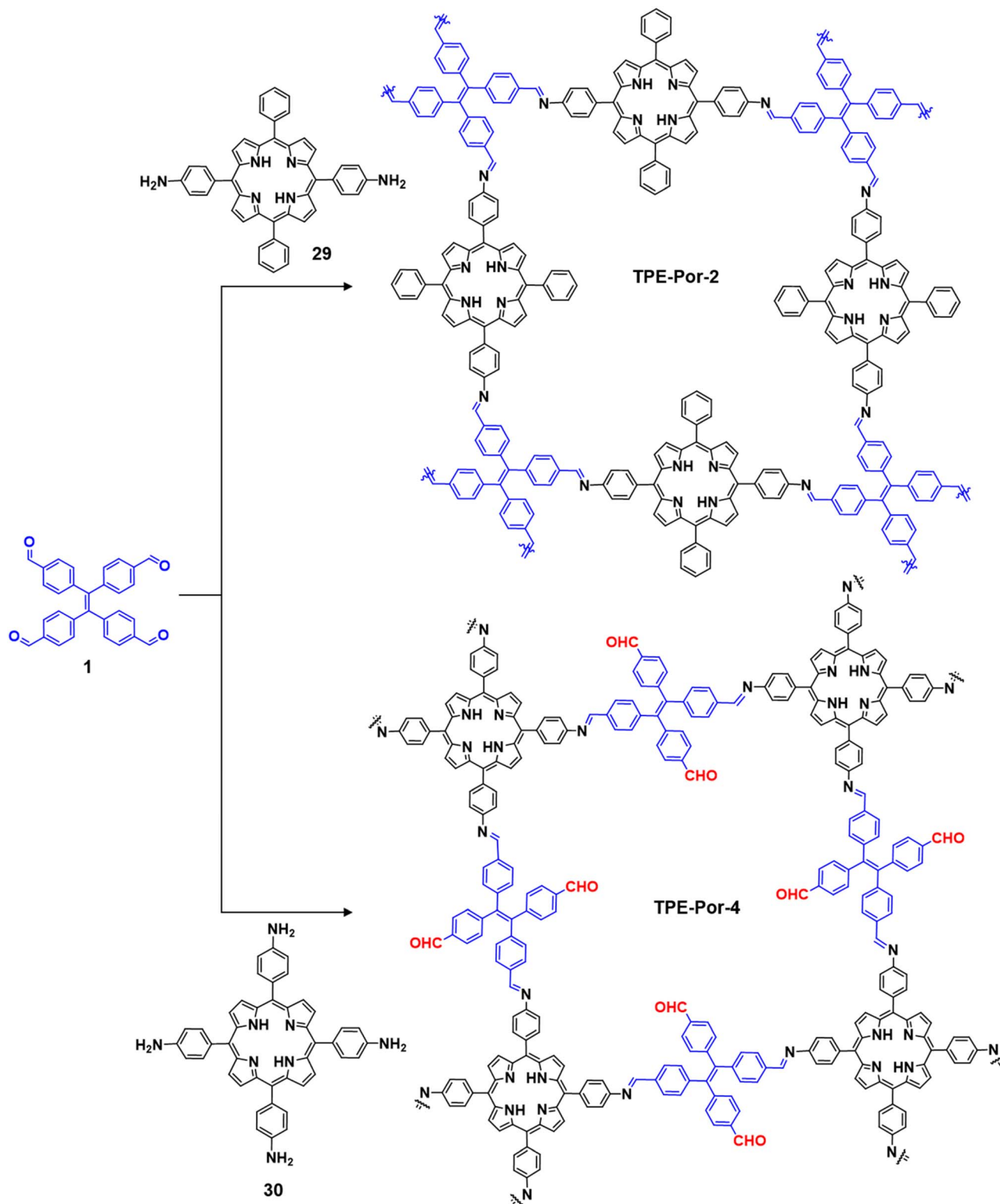
Fig. 21 Synthesis of the porphyrin-based COFs **TPE-Por-2** and **TPRE-Por-4**.

respectively. **TPE-Por-4,** due to its better dispersibility, was chosen for investigating the changes in its fluorescence with variations in pH, and typical response was observed in the pH range of 4.15–2.01. At pH <2, a very distinct emission color change from dark red to bright green was observed. This behaviour most likely emerged from the protonation of pyrrole nitrogen of porphyrin rings at low pH.

26360 | *J. Mater. Chem. A*, 2023, **11**, 26340–26370

This journal is © The Royal Society of Chemistry 2023

4. Conclusions

Apart from tunable porosity and high physicochemical stability, their capability to form new topologies and accommodate diverse active functional groups within their pores makes these COFs interesting in terms of new properties and diverse applications. Selective transformations of seemingly similar functional groups during the synthesis of imine-linked COF were effected *via* protection, post synthetic modification, ligand exchange and site-selective synthesis. However, sub-stoichiometric synthesis of Type III COFs that shows a high degree of tolerance to chemically equivalent reactive sites and yields the products *via* orthogonal reactions is a recent development. The unusual selectivity observed during sub-stoichiometric synthesis of COFs not only widens their applications but assists in obtaining a better understanding of the general pathways behind COF formation. The literature reports on COFs synthesized through the sub-stoichiometric approach, including their topologies, linkages and applications are summarized in Table 1. Though several reports on the synthesis and applications of Type-III COFs have emerged over the last five years, extension to other linkages is still in its infancy. Therefore, we believe that this approach provides enough opportunities and challenges for focussed research in terms of new linkages, monomeric units, topologies, and applications.

5. Future prospects

While COFs, in general, and sub-stoichiometric COFs, in particular, have shown a wide range of applications emanating from their structural attributes, Type III COFs have the additional advantage of having the periodic presence of unreacted heteroatomic functional groups. Such active functional groups benefit from the possibilities for further chemical modifications, specific interactions with ions/molecules, catalysis, energy storage, *etc.*, while retaining long-range order and crystallinity, robustness, and porosity. These unique prospects of type III COFs that retain the advantages of stoichiometric COFs lead to improved properties and applications that are otherwise difficult in conventional COFs.

The sub-stoichiometric approach is a synthetic tool in terms of generating more functionalities in COFs aiming at unique properties and applications. Although Type III COFs present an interesting scenario for further exploration in terms of practical applicability, the field is still in its infancy.[170] In this section, we discuss the possible ways to expand the use of monomers, linkages and topologies, multicomponent approaches, polymorphism, isomerism, modifications in physicochemical properties, practical applicability as a synthetic tool, and new avenues for applications.

5.1 Extending to new linkages and monomers

Type III COFs are generally stoichiometry-controlled products, and reaction conditions including solvents and temperature are as critical as the choice of monomers. While the majority of the reports are based on Schiff base chemistry leading to imine-linked Type III COFs, there is only a single report with an olefin linkage.[151] This observation suggests that the sub-stoichiometric approach can be extended to new or existing linkages, resulting in COFs with periodic arrays of various functional groups. Covalent and non-covalent chemistry of the active functional groups in these COFs allows for further structural diversification and improvement in properties. This also calls for the identification of new monomeric units for the generation of COFs with new and stable linkages.

5.2 Exploration of new topologies and multicomponent reactions

Though several reports hypothesized COF formation mechanisms, unknown aspects behind covalent bond crystallisation can be better revealed by exploring Type III COFs. The structural and functional complexities are enhanced in COFs synthesized *via* the sub-stoichiometric approach. While a good number of existing reports on sub-stoichiometric COFs are hypothesis-driven in terms of structural elucidation, attempts using combinations of monomers of various symmetry combined with the efforts on crystallography, theoretical modelling, and X-ray and electron diffraction techniques are expected to result in reliable predictions of the resulting unconventional topologies.[171]

While the realization of new topologies and elucidating the exact structure of COFs may not be straightforward, *bex* topology alone has a lot to offer.[34] As discussed above, this field has so far witnessed the use of the combination of only tetratopic and tritopic/tetratopic/hexatopic monomers to yield 2D and 3D COFs. Use of other tritopic or tetratopic monomers expected to yield only *bex* topology makes theoretical predictions and structural elucidations facile. Working with defined topologies also helps to understand the role of flexible cores and bifunctional group containing monomers in deciding the final structure of the COFs.

In addition, synthesis of 1D COFs *via* sub-stoichiometric approaches and subsequent crosslinking to the corresponding 2D architecture, yielding dual linked COFs, is yet another less explored but interesting area for investigation.[35] These 1D chains can be effectively wrapped over nanotubes, or other nanostructures through covalent linkages, which could possibly yield new hybrid materials with interesting properties. Extending such approaches to 2D COFs results in diverse porous materials or hybrids with unprecedented structural and functional complexities.

Lotsch and co-workers have also demonstrated that replacing a tetratopic linker with a ditopic linker can generate all-linked analogues of sub-stoichiometric COFs.[34] Such an approach is yet to be attempted in other sub-stoichiometric COFs. This approach could possibly be viewed as a strategy to construct all-linked *bex* topology with [4 + 3 + 2] linkages or sub-stoichiometric COFs with [4 + 3 + 4] linkages. In the latter case, one of the tetratopic linkers selectively behaves as a ditopic linker in generating sub-stoichiometric COFs with two different tetratopic linkers in the framework. Such attempts are

This journal is © The Royal Society of Chemistry 2023

J. Mater. Chem. A, 2023, **11**, 26340–26370 | **26361**

Table 1 Reported sub-stoichiometric COFs, synthetic approaches, topologies, linkages, and applications

Linker 1	Linker 2	Topology	Application	Ref.
1	**2**	*Rhombic*	CO_2 absorption	116
4		*tth defect*	Photocatalysis	150
7		*sql*		134
7		*tth defect*		117
27		*Rhombic*	Photocatalysis	152

26362 | *J. Mater. Chem. A*, 2023, **11**, 26340–26370

This journal is © The Royal Society of Chemistry 2023

Table 1 (*Contd.*)
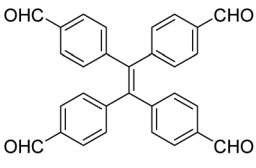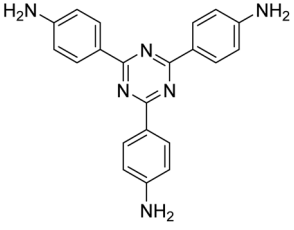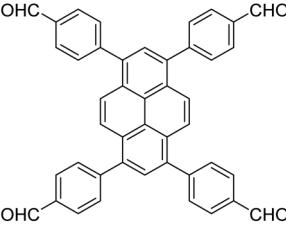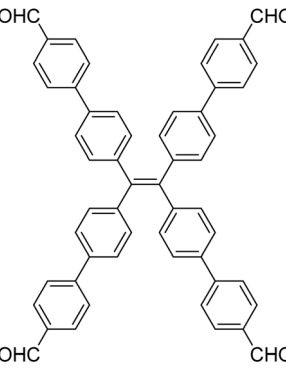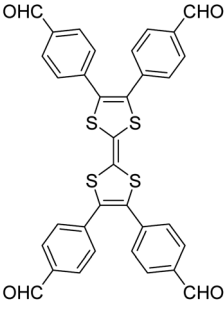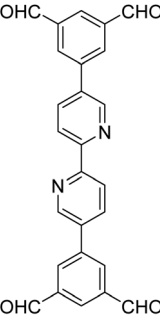
Linker 1	Linker 2	Topology	Application	Ref.
1	**18**	*bex*	Photocatalysis	150
			Li–S battery	167
10		*bex*	Water sensing and harvesting	148
16		*bex*	Photocatalysis	150
			Photodetector	168
			Li–S battery	167
25		*bex*	Photocatalysis	37
26		*bex*	Photocatalysis	133

This journal is © The Royal Society of Chemistry 2023

J. Mater. Chem. A, 2023, **11**, 26340–26370 | **26363**
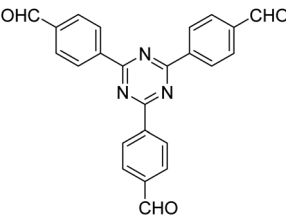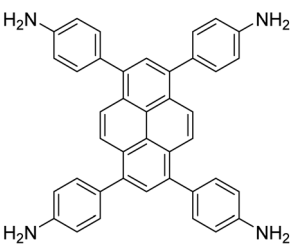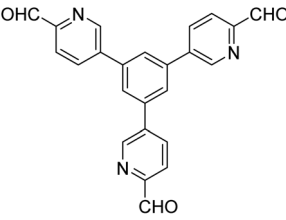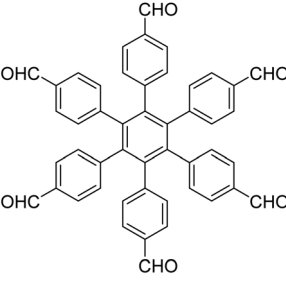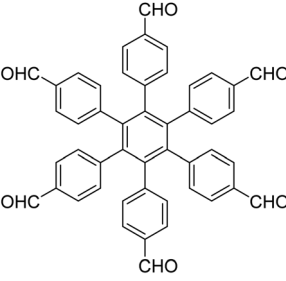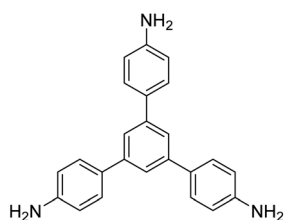
Table 1 (*Contd.*)

Linker 1	Linker 2	Topology	Application	Ref.
4	**3**	*bex*	CO_2 adsorption Catalysis	34
5				
7	**12**	*pts*	Gas adsorption and separation	118
	9	*hcb*		

26364 | *J. Mater. Chem. A*, 2023, **11**, 26340–26370

This journal is © The Royal Society of Chemistry 2023

Table 1 (*Contd.*)
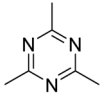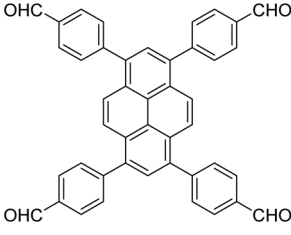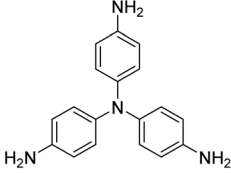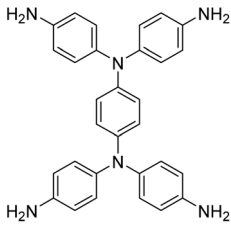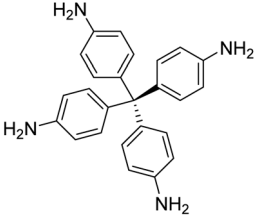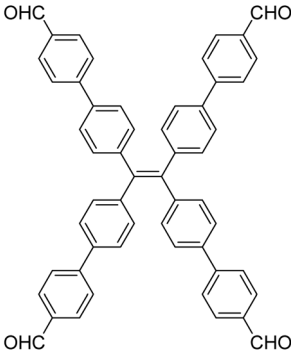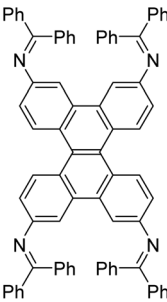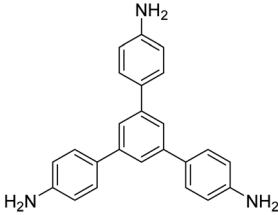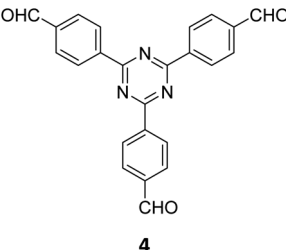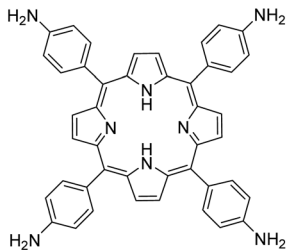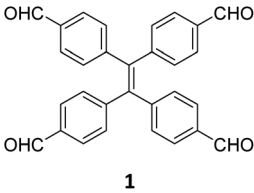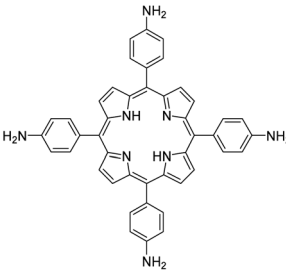
Linker 1	Linker 2	Topology	Application	Ref.
10	**22**	*bex*	Photocatalysis	151
	11	*1D COF*	Dual linked 2D COFs	35
	19	*Rhombic*	Iodine adsorption	149
14	**13**	*dia*	Heterogeneous Catalysis	36
16	**15**	*Rhombic*	CO_2 and H_2O absorption	138
	9	*bex*	Dye removal	166

This journal is © The Royal Society of Chemistry 2023

J. Mater. Chem. A, 2023, **11**, 26340–26370 | **26365**

Table 1 (*Contd.*)

Linker 1	Linker 2	Topology	Application	Ref.
4	**28**	*bex*	Photocatalysis	153
1	**30**	*Rhombic*	pH response	169

envisioned to result in COFs with tuneable photochemical and electro-optical characteristics.

5.3 Isomerism and polymorphism

While reticular chemistry has led to significant progress in the development of framework materials, practical realization of isomeric COFs has not been explored extensively. Dimensional isomers are generally constructed from the same building blocks under different reaction conditions, but extend in different dimensions (2D or 3D).[172] Different orientations of the molecular building blocks in these isomeric frameworks alter their physicochemical properties and functions. Isomerization in COFs is a recently realized phenomenon where the influence of solvent and/or temperature yielding different isomers and can also be extended to type-III COFs.[173] Conversion of a kinetic product to a stable thermodynamic product suggests that transformation of sub-stoichiometric COFs to all-linked COFs (Type III to Type I) could also possibly be achieved particularly for rhombic topologies. This two-step process may yield better surface area and/or crystallinity, which is yet to be demonstrated. This could also provide a new synthetic methodology that attempts to impart kinetic/thermodynamic stability to COFs or to achieve both types of COFs in a continuous flow system[174,175] where the isomers are obtained just by controlling the monomer feed ratio, solvent compositions or temperature. The sub-stoichiometric approach is probably the most practical strategy for the creation of such isomers of COFs using flexible monomers, with a multitude of active functionalities within the framework structure, though such reports are rarely found.

Since the first report on sub-stoichiometric COFs, there are only three instances of polymorphism reported.[116,149,152] These reports on Type III COFs involve the use of tetratopic monomers and rhombic topologies. In these attempts, COFs with unreacted carbonyls were realized just by changing the solvent(s) rather than the stoichiometry of the monomers. Unlike other topologies dealt with in sub-stoichiometric COFs, the rhombic topology allows the exclusive generation of polymorphic COFs using different solvent combinations, while the ratio of starting monomeric linkers remains unaltered. Though these are not strictly sub-stoichiometric syntheses where variations in stoichiometry of the monomers result in unreacted functional groups in the COF structure, we have deliberately included these reports in this review, since the resulting COFs are indeed Type III with active functional groups.

5.4 As a synthetic tool

The reversible nature of the linkages in COFs can be utilized for selective functional group interconversions. Unreacted functional groups of sub-stoichiometric COFs can undergo post synthetic modifications. The resulting COFs in principle can be promoted to undergo transamination reactions to yield an all-linked COF and diagonally functionalized aldehydes or amines. This approach, if realized, is envisioned to provide a useful synthetic tool to generate organic molecules which are difficult to be obtained *via* selective functionalization in their monomeric states. Moreover, reconstruction strategies, as reported by Cooper and co-workers, *via* "the pre-organization of monomers using a reversible and removable covalent tether, followed by confined

26366 | *J. Mater. Chem. A*, 2023, **11**, 26340–26370

This journal is © The Royal Society of Chemistry 2023

polymerization"[176] present a yet another promising avenue for sub-stoichiometric synthesis towards realizing stable and crystalline COFs with active functionalities for further modifications.

5.5 Avenues for new applications

Broadening the scope and applicability of COFs demands unique structural diversity and pertinent functionalities that are exigent *via* conventional synthetic approaches. Though post-synthetic modification provides an option to achieve such diversification of COF architectures, the choices are limited by strictly orthogonal reaction requirements. We have elaborated the applications of Type III COFs in Section 3.3 of this article. While these are not an exhaustive list of applications of this class of COFs, we expect that concerted efforts from the research community working on these materials with emerging linkages, monomers and topologies combined with advancements in structural characterization tools would result in a large realm of applications in the near future.

Author contributions

SV and SS wrote the manuscript. AA and SS conceptualized and supervised the project. AA and SS reviewed and edited the manuscript. All authors approved the submission of the reviewed draft.

Conflicts of interest

There are no conflicts to declare.

Acknowledgements

Notes and references

1 A. R. Brill, E. Koren and G. de Ruiter, *J. Mater. Chem. C*, 2021, **9**, 11569–11587.

2 M. Franz, S. Chandola, M. Koy, R. Zielinski, H. Aldahhak, M. Das, M. Freitag, U. Gerstmann, D. Liebig, A. K. Hoffmann, M. Rosin, W. G. Schmidt, C. Hogan, F. Glorius, N. Esser and M. Dähne, *Nat. Chem.*, 2021, **13**, 828–835.

3 Take aim (Editorial), *Nat. Chem.*, 2012, **4**, 955.

4 P. M. Tadross and E. N. Jacobsen, *Nat. Chem.*, 2012, **4**, 963–965.

5 A. A. Bastian, A. Marcozzi and A. Herrmann, *Nat. Chem.*, 2012, **4**, 789–793.

6 S. K. Silverman, *Nat. Chem.*, 2012, **4**, 774–775.

7 I. S. Young and P. S. Baran, *Nat. Chem.*, 2009, **1**, 193–205.

8 Z. Huang and G. Dong, *Acc. Chem. Res.*, 2017, **50**, 465–471.

9 B. C. Wilcock, B. E. Uno, G. L. Bromann, M. J. Clark, T. M. Anderson and M. D. Burke, *Nat. Chem.*, 2012, **412**(4), 996–1003.

10 P. A. Lichtor and S. J. Miller, *Nat. Chem.*, 2012, **412**(4), 990–995.

11 C. Hui, F. Chen, F. Pu and J. Xu, *Nat. Rev. Chem*, 2019, **32**(3), 85–107.

12 T. Newhouse, P. S. Baran and R. W. Hoffmann, *Chem. Soc. Rev.*, 2009, **38**, 3010–3021.

13 G. Sartori, R. Ballini, F. Bigi, G. Bosica, R. Maggi and P. Righi, *Chem. Rev.*, 2004, **104**, 199–250.

14 I. S. Young and P. S. Baran, *Nat. Chem.*, 2009, **13**(1), 193–205.

15 W. Lu, Z. Wei, Z. Y. Gu, T. F. Liu, J. Park, J. Park, J. Tian, M. Zhang, Q. Zhang, T. Gentle, M. Bosch and H. C. Zhou, *Chem. Soc. Rev.*, 2014, **43**, 5561–5593.

16 A. J. Howarth, Y. Liu, P. Li, Z. Li, T. C. Wang, J. T. Hupp and O. K. Farha, *Nat. Rev. Mater.*, 2016, **1**, 1–15.

17 N. Hanikel, M. S. Prévot and O. M. Yaghi, *Nat. Nanotechnol.*, 2020, **15**, 348–355.

18 Z. Ji, H. Wang, S. Canossa, S. Wuttke and O. M. Yaghi, *Adv. Funct. Mater.*, 2020, **30**, 2000238.

19 R. Freund, O. Zaremba, G. Arnauts, R. Ameloot, G. Skorupskii, M. Dincă, A. Bavykina, J. Gascon, A. Ejsmont, J. Goscianska, M. Kalmutzki, U. Lächelt, E. Ploetz, C. S. Diercks and S. Wuttke, *Angew. Chem., Int. Ed.*, 2021, **60**, 23975–24001.

20 C. S. Diercks and O. M. Yaghi, *Science*, 2017, **355**, eaal1585.

21 N. Huang, P. Wang and D. L. Jiang, *Nat. Rev. Mater.*, 2016, **1**, 16068.

22 S. J. Lyle, P. J. Waller and O. M. Yaghi, *Trends Chem.*, 2019, **1**, 172–184.

23 H. Wang, Y. Yang, X. Yuan, W. L. Teo, Y. Wu, L. Tang and Y. Zhao, *Mater. Today*, 2022, **53**, 106–133.

24 A. M. Evans, M. J. Strauss, A. R. Corcos, Z. Hirani, W. Ji, L. S. Hamachi, X. Aguilar-Enriquez, A. D. Chavez, B. J. Smith and W. R. Dichtel, *Chem. Rev.*, 2022, **122**, 442–564.

25 X. Guan, F. Chen, S. Qiu and Q. Fang, *Angew. Chem., Int. Ed.*, 2023, **62**, e202213203.

26 J. Jiang, Y. Zhao and O. M. Yaghi, *J. Am. Chem. Soc.*, 2016, **138**, 3255–3265.

27 S. Kandambeth, K. Dey and R. Banerjee, *J. Am. Chem. Soc.*, 2019, **141**, 1807–1822.

28 X. Chen, K. Geng, R. Liu, K. T. Tan, Y. Gong, Z. Li, S. Tao, Q. Jiang and D. Jiang, *Angew. Chem., Int. Ed.*, 2020, **59**, 5050–5091.

29 L. Deng, Z. Ding, X. Ye and D. Jiang, *Acc. Mater. Res.*, 2022, **3**, 879–893.

30 J. L. Segura, S. Royuela and M. Mar Ramos, *Chem. Soc. Rev.*, 2019, **48**, 3903–3945.

31 X. Huang, C. Sun and X. Feng, *Sci. China: Chem.*, 2020, **63**, 1367–1390.

32 Y. Li, W. Chen, G. Xing, D. Jiang and L. Chen, *Chem. Soc. Rev.*, 2020, **49**, 2852–2868.

33 H. Ding, A. Mal and C. Wang, *Mater. Chem. Front.*, 2020, **4**, 113–127.

This journal is © The Royal Society of Chemistry 2023

J. Mater. Chem. A, 2023, **11**, 26340–26370 | **26367**

34 T. Banerjee, F. Haase, S. Trenker, B. P. Biswal, G. Savasci, V. Duppel, I. Moudrakovski, C. Ochsenfeld and B. V. Lotsch, *Nat. Commun.*, 2019, **10**, 2689.

35 H. L. Nguyen, C. Gropp and O. M. Yaghi, *J. Am. Chem. Soc.*, 2020, **142**, 2771–2776.

36 C. Xu, J. Lin, D. Yan, Z. Guo, D. J. Austin, H. Zhan, A. Kent and Y. Yue, *ACS Appl. Nano Mater.*, 2020, **3**, 6416–6422.

37 M. Lu, M. Zhang, J. Liu, T.-Y. Yu, J.-N. Chang, L.-J. Shang, S.-L. Li and Y.-Q. Lan, *J. Am. Chem. Soc.*, 2022, **144**, 1861–1871.

38 K. Geng, T. He, R. Liu, S. Dalapati, K. T. Tan, Z. Li, S. Tao, Y. Gong, Q. Jiang and D. Jiang, *Chem. Rev.*, 2020, **120**, 8814–8933.

39 L. Bourda, C. Krishnaraj, P. Van Der Voort and K. Van Hecke, *Mater. Adv.*, 2021, **2**, 2811–2845.

40 C. Gropp, S. Canossa, S. Wuttke, F. Gándara, Q. Li, L. Gagliardi and O. M. Yaghi, *ACS Cent. Sci.*, 2020, **6**, 1255–1273.

41 K. T. Tan, S. Ghosh, Z. Wang, F. Wen, D. Rodríguez-San-Miguel, J. Feng, N. Huang, W. Wang, F. Zamora, X. Feng, A. Thomas and D. Jiang, *Nat. Rev. Methods Primers*, 2023, **3**, 1.

42 H. Lyu, Z. Ji, S. Wuttke and O. M. Yaghi, *Chem*, 2020, **6**, 2219–2241.

43 F. Haase and B. V. Lotsch, *Chem. Soc. Rev.*, 2020, **49**, 8469–8500.

44 J. Hu, Z. Huang and Y. Liu, *Angew. Chem., Int. Ed.*, 2023, **62**, e202306999.

45 L. Bourda, C. Krishnaraj, P. Van Der Voort and K. Van Hecke, *Mater. Adv.*, 2021, **2**, 2811–2845.

46 A. R. Bagheri and N. Aramesh, *J. Mater. Sci.*, 2021, **56**, 1116–1132.

47 H. S. Sasmal, A. Kumar Mahato, P. Majumder and R. Banerjee, *J. Am. Chem. Soc.*, 2022, **144**, 11482–11498.

48 S. Karak, K. Dey and R. Banerjee, *Adv. Mater.*, 2022, **34**, 2202751.

49 S. Xu, M. Richter and X. Feng, *Acc. Mater. Res.*, 2021, **2**, 252–265.

50 F. Guo, W. Zhang, S. Yang, L. Wang and G. Yu, *Small*, 2023, 2207876.

51 Q. Guan, L. Zhou and Y. Dong, *J. Am. Chem. Soc.*, 2023, **145**, 1475–1496.

52 H. Yazdani, S. E. Hooshmand and R. S. Varma, *Org. Chem. Front.*, 2022, **9**, 4178–4191.

53 Y. Yusran, X. Guan, H. Li, Q. Fang and S. Qiu, *Natl. Sci. Rev.*, 2020, **7**, 170–190.

54 K. S. Song, P. W. Fritz and A. Coskun, *Chem. Soc. Rev.*, 2022, **51**, 9831–9852.

55 X. Wang, H. Liu, J. Zhang and S. Chen, *Polym. Chem.*, 2023, **14**, 1293–1317.

56 H. Li, A. Dilipkumar, S. Abubakar and D. Zhao, *Chem. Soc. Rev.*, 2023, **52**, 6294–6329.

57 B. Chen, H. Xie, L. Shen, Y. Xu, M. Zhang, M. Zhou, B. Li, R. Li and H. Lin, *Small*, 2023, **19**, 2207313.

58 Y. Yuan, K. T. Bang, R. Wang and Y. Kim, *Adv. Mater.*, 2023, **35**, 1–26.

59 C. Yuan, Z. Wang, W. Xiong, Z. Huang, Y. Lai, S. Fu, J. Dong, A. Duan, X. Hou, L. Yuan and Y. Cui, *J. Am. Chem. Soc.*, 2023, **145**, 18956–18967.

60 L. Liu, Y. Hu, S. Huang, Y. Jin, J. Cui, W. Gong and W. Zhang, *Chem. Sci.*, 2021, **12**, 13316–13320.

61 L. Wei, T. Sun, Z. Shi, Z. Xu, W. Wen, S. Jiang, Y. Zhao, Y. Ma and Y. B. Zhang, *Nat. Commun.*, 2022, **13**, 1–10.

62 Z. Meng and K. A. Mirica, *Chem. Soc. Rev.*, 2021, **50**, 13498–13558.

63 T. Skorjanc, D. Shetty and M. Valant, *ACS Sens.*, 2021, **6**, 1461–1481.

64 Y. Qian, J. Li, M. Ji, J. Li, D. Ma, A. Liu, Y. Zhao and C. Yang, *Front. Chem.*, 2022, **10**, 1–7.

65 Y. Wei, W. Yang and H. Guo, *ChemistrySelect*, 2023, **8**, e202301828.

66 J. Yu, L. Luo, H. Shang and B. Sun, *Biosensors*, 2023, **13**, 636.

67 R. Xue, Y.-S. Liu, S.-L. Huang and G.-Y. Yang, *ACS Sens.*, 2023, **8**, 2124–2148.

68 E. Martínez-periñán, M. Martínez-fernández, J. L. Segura and E. Lorenzo, *Sensors*, 2022, **22**, 1–29.

69 X. Li and K. P. Loh, *ACS Mater. Lett.*, 2019, **1**, 327–335.

70 H. Salemi, M. Debruyne, V. Van Speybroeck, P. Van Der Voort, M. D'hooghe and C. V. Stevens, *J. Mater. Chem. A*, 2022, **10**, 20707–20729.

71 E. Nikkhoo, S. Mallakpour and C. M. Hussain, *New J. Chem.*, 2023, **47**, 6765–6788.

72 J. Guo and D. Jiang, *ACS Cent. Sci.*, 2020, **6**, 869–879.

73 H. Chen, H. S. Jena, X. Feng, K. Leus and P. van der Voort, *Angew. Chem., Int. Ed.*, 2022, **61**, e202204938.

74 T. He and Y. Zhao, *Angew. Chem., Int. Ed.*, 2023, **62**, e202303086.

75 K. Prakash, B. Mishra, D. D. Díaz, C. M. Nagaraja and P. Pachfule, *J. Mater. Chem. A*, 2023, 14489–14538.

76 S. Bommakanti, A. Puthukkudi, M. Samal, P. Sahu and B. P. Biswal, *Cryst. Growth Des.*, 2023, **23**, 6172–6200.

77 X. Zhao, P. Pachfule and A. Thomas, *Chem. Soc. Rev.*, 2021, **50**, 6871–6913.

78 H. L. Nguyen, *Adv. Mater.*, 2023, **35**, 1–7.

79 C. Sun, D. Sheng, B. Wang and X. Feng, *Angew. Chem., Int. Ed.*, 2023, **62**, 202303378.

80 J. L. Segura, M. J. Mancheño and F. Zamora, *Chem. Soc. Rev.*, 2016, **45**, 5635–5671.

81 I. Janica, V. Patroniak, P. Samorì and A. Ciesielski, *Chem. – Asian J.*, 2018, **13**, 465–481.

82 L.-J. Wang, P.-Y. Dong, G. Zhang and F.-M. Zhang, *Energy Fuels*, 2023, **37**, 6323–6347.

83 C. Qian, L. Feng, W. L. Teo, J. Liu, W. Zhou, D. Wang and Y. Zhao, *Nat. Rev. Chem*, 2022, **6**, 881–898.

84 B. P. Biswal, S. Chandra, S. Kandambeth, B. Lukose, T. Heine and R. Banerjee, *J. Am. Chem. Soc.*, 2013, **135**, 5328–5331.

85 M. Matsumoto, R. R. Dasari, W. Ji, C. H. Feriante, T. C. Parker, S. R. Marder and W. R. Dichtel, *J. Am. Chem. Soc.*, 2017, **139**, 4999–5002.

86 B. Díaz de Greñu, J. Torres, J. García-González, S. Muñoz-Pina, R. de los Reyes, A. M. Costero, P. Amorós and J. V. Ros-Lis, *ChemSusChem*, 2021, **14**, 208–233.

26368 | *J. Mater. Chem. A*, 2023, **11**, 26340–26370

This journal is © The Royal Society of Chemistry 2023

87 B. J. Smith, L. R. Parent, A. C. Overholts, P. A. Beaucage, R. P. Bisbey, A. D. Chavez, N. Hwang, C. Park, A. M. Evans, N. C. Gianneschi and W. R. Dichtel, *ACS Cent. Sci.*, 2017, **3**, 58–65.

88 D. W. Burke, C. Sun, I. Castano, N. C. Flanders, A. M. Evans, E. Vitaku, D. C. McLeod, R. H. Lambeth, L. X. Chen, N. C. Gianneschi and W. R. Dichtel, *Angew. Chem., Int. Ed.*, 2020, **132**, 5203–5209.

89 L. Cusin, H. Peng, A. Ciesielski and P. Samorì, *Angew. Chem., Int. Ed.*, 2021, **60**, 14236–14250.

90 X. Guan, Q. Fang, Y. Yan and S. Qiu, *Acc. Chem. Res.*, 2022, **55**, 1912–1927.

91 L. Cusin, H. Peng, A. Ciesielski and P. Samorì, *Angew. Chem., Int. Ed.*, 2021, **60**, 14236–14250; G. Jiang, W. Zou, Z. Ou, W. Zhang, Z. Liang and L. Du, *Chem. –Eur. J.*, 2023, **29**, e202203610.

92 A. M. Evans, L. R. Parent, N. C. Flanders, R. P. Bisbey, E. Vitaku, M. S. Kirschner, R. D. Schaller, L. X. Chen, N. C. Gianneschi and W. R. Dichtel, *Science*, 2018, **361**, 52–57.

93 C. Feriante, A. M. Evans, S. Jhulki, I. Castano, M. J. Strauss, S. Barlow, W. R. Dichtel and S. R. Marder, *J. Am. Chem. Soc.*, 2020, **142**, 18637–18644.

94 I. Castano, A. M. Evans, H. Li, E. Vitaku, M. J. Strauss, J. L. Brédas, N. C. Gianneschi and W. R. Dichtel, *ACS Cent. Sci.*, 2019, **5**, 1892–1899.

95 H. Li, A. M. Evans, I. Castano, M. J. Strauss, W. R. Dichtel and J. L. Bredas, *J. Am. Chem. Soc.*, 2020, **142**, 1367–1374.

96 L. Deng, X. Kang, T. Quan, L. Yang, S. Liu, K. Zhang, M. Gao, Z. Xia and D. Gao, *ACS Appl. Mater. Interfaces*, 2021, **13**, 33449–33463.

97 S. T. Emmerling, L. S. Germann, P. A. Julien, I. Moudrakovski, M. Etter, T. Friščić, R. E. Dinnebier and B. V. Lotsch, *Chem*, 2021, **7**, 1639–1652.

98 Q. Guan, D. D. Fu, Y. A. Li, X. M. Kong, Z. Y. Wei, W. Y. Li, S. J. Zhang and Y. Bin Dong, *iScience*, 2019, **14**, 180–198.

99 Z. Guo, H. Wu, Y. Chen, S. Zhu, H. Jiang, S. Song, Y. Ren, Y. Wang, X. Liang, G. He, Y. Li and Z. Jiang, *Angew. Chem., Int. Ed.*, 2022, **61**, e202210466.

100 Z. Li, Z. W. Liu, Z. Li, T. X. Wang, F. Zhao, X. Ding, W. Feng and B. H. Han, *Adv. Funct. Mater.*, 2020, **30**, 1–9.

101 K. Kaya, D. Ditz, A. Jaworski, J. Chen, S. Monti, G. Barcaro, S. Budnyk, A. Slabon and R. Palkovits, *Adv. Sustainable Syst.*, 2023, **7**, 2300071.

102 N. Huang, R. Krishna and D. Jiang, *J. Am. Chem. Soc.*, 2015, **137**, 7079–7082.

103 M. S. Lohse, T. Stassin, G. Naudin, S. Wuttke, R. Ameloot, D. De Vos, D. D. Medina and T. Bein, *Chem. Mater.*, 2016, **28**, 626–631.

104 W. Ji, L. Xiao, Y. Ling, C. Ching, M. Matsumoto, R. P. Bisbey, D. E. Helbling and W. R. Dichtel, *J. Am. Chem. Soc.*, 2018, **140**, 12677–12681.

105 X. Guan, H. Li, Y. Ma, M. Xue, Q. Fang, Y. Yan, V. Valtchev and S. Qiu, *Nat. Chem.*, 2019, **11**, 587–594.

106 H. L. Qian, Y. Li and X. P. Yan, *J. Mater. Chem. A*, 2018, **6**, 17307–17311.

107 E. Dautzenberg, G. Li and L. C. P. M. de Smet, *ACS Appl. Mater. Interfaces*, 2023, **15**, 5118–5127.

108 S. Y. Zhang, X. H. Tang, Y. L. Yan, S. Q. Li, S. Zheng, J. Fan, X. Li, W. G. Zhang and S. Cai, *ACS Macro Lett.*, 2021, **10**, 1590–1596.

109 Z. Dong, Y. Yang, X. Cai, X. Tang, Y. Yan, S. Zheng, W. Zhang, S. Cai and J. Fan, *J. Solid State Chem.*, 2022, **316**, 123644.

110 Y. Zhao, X. Xu, C. Xu, D. Meng, X. Liang and J. Qiu, *New J. Chem.*, 2022, **46**, 11980–11984.

111 X. Tang, Y. Yang, X. Li, X. Wang, D. Guo, S. Zhang, K. Zhang, J. Wu, J. Zheng, S. Zheng, J. Fan, W. Zhang and S. Cai, *ACS Appl. Mater. Interfaces*, 2023, **15**(20), 24836–24845.

112 Y. Y. Wen, Z. Y. Dong, X. H. Tang, W. G. Zhang, S. L. Cai and J. Fan, *New J. Chem.*, 2023, **47**, 19039–19046.

113 X. Li, Z. Jia, J. Zhang, Y. Zou, Y. Zhang, K. Shu, W. Liu, N. Liu, Y. Li and L. Ma, *Small*, 2023, **19**, 2303775.

114 Y. Liang, L. Feng, X. Liu, Y. Zhao, Q. Chen, Z. Sui and N. Wang, *Chem. Eng. J.*, 2021, **404**, 127095.

115 R. Liu, L. Huang, H. Tao, X. Lei and Q. Shuai, *J. Environ. Chem. Eng.*, 2022, **10**, 107300.

116 Q. Gao, X. Li, G. Ning, H. Xu, C. Liu, B. Tian, W. Tang and K. P. Loh, *Chem. Mater.*, 2018, **30**, 1762–1768.

117 B. Zhang, H. Mao, R. Matheu, J. A. Reimer, S. A. Alshmimri, S. Alshihri and O. M. Yaghi, *J. Am. Chem. Soc.*, 2019, **141**, 11420–11424.

118 L. Chen, C. Gong, X. Wang, F. Dai, M. Huang, X. Wu, C. Z. Lu and Y. Peng, *J. Am. Chem. Soc.*, 2021, **143**, 10243–10249.

119 A. G. Slater and A. I. Cooper, *Science*, 2015, **348**, aaa8075.

120 K. Shen, L. Zhang, X. Chen, L. Liu, D. Zhang, Y. Han, J. Chen, J. Long, R. Luque, Y. Li and B. Chen, *Science*, 2018, **359**, 206–210.

121 H. Li, J. Ding, X. Guan, F. Chen, C. Li, L. Zhu, M. Xue, D. Yuan, V. Valtchev, Y. Yan, S. Qiu and Q. Fang, *J. Am. Chem. Soc.*, 2020, **142**, 13334–13338.

122 M. E. Davis, *Nature*, 2002, **417**, 813–821.

123 T. Liu, Y. Zhao, M. Song, X. Pang, X. Shi, J. Jia, L. Chi and G. Lu, *J. Am. Chem. Soc.*, 2023, **145**, 2544–2552.

124 S. Kandambeth, V. Venkatesh, D. B. Shinde, S. Kumari, A. Halder, S. Verma and R. Banerjee, *Nat. Commun.*, 2015, **6**, 6786.

125 Y. Y. Liu, X. C. Li, S. Wang, T. Cheng, H. Yang, C. Liu, Y. Gong, W. Y. Lai and W. Huang, *Nat. Commun.*, 2020, **11**, 1–8.

126 H. Hong, J. Liu, H. Huang, C. Atangana Etogo, X. Yang, B. Guan and L. Zhang, *J. Am. Chem. Soc.*, 2019, **141**, 14764–14771.

127 A. K. Mohammed, S. Usgaonkar, F. Kanheerampockil, S. Karak, A. Halder, M. Tharkar, M. Addicoat, T. G. Ajithkumar and R. Banerjee, *J. Am. Chem. Soc.*, 2020, **142**, 8252–8261.

128 S. Y. Ding and W. Wang, *Chem. Soc. Rev.*, 2013, **42**, 548–568.

129 M. X. Wu and Y. W. Yang, *Chin. Chem. Lett.*, 2017, **28**, 1135–1143.

130 G. Barin, V. Krungleviciute, O. Gutov, J. T. Hupp, T. Yildirim and O. K. Farha, *Inorg. Chem.*, 2014, **53**, 6914–6919.

This journal is © The Royal Society of Chemistry 2023

J. Mater. Chem. A, 2023, **11**, 26340–26370 | **26369**

131 Z. Fang, B. Bueken, D. E. De Vos and R. A. Fischer, *Angew. Chem., Int. Ed.*, 2015, **54**, 7234–7254.

132 J. Ren, M. Ledwaba, N. M. Musyoka, H. W. Langmi, M. Mathe, S. Liao and W. Pang, *Coord. Chem. Rev.*, 2017, **349**, 169–197.

133 Y. Liu, W. K. Han, W. Chi, Y. Mao, Y. Jiang, X. Yan and Z. G. Gu, *Appl. Catal., B*, 2023, **331**, 122691.

134 N. He, B. Liu, B. Jiang, X. Li, Z. Jia, J. Zhang, H. Long, Y. Zhang, Y. Zou, Y. Yang, S. Xiong, K. Cao, Y. Li and L. Ma, *ACS Appl. Mater. Interfaces*, 2023, **15**, 16975–16983.

135 K. Gottschling, L. Stegbauer, G. Savasci, N. A. Prisco, Z. J. Berkson, C. Ochsenfeld, B. F. Chmelka and B. V. Lotsch, *Chem. Mater.*, 2019, **31**, 1946–1955.

136 M. Yin, L. Wang and S. Tang, *ACS Appl. Mater. Interfaces*, 2022, **14**, 55674–55685.

137 H. Lyu, H. Li, N. Hanikel, K. Wang and O. M. Yaghi, *J. Am. Chem. Soc.*, 2022, **144**, 12989–12995.

138 X. Yang, Z. Xie, T. Zhang, G. Zhang, Z. Zhao, Y. Wang, G. Xing and L. Chen, *Sci. China: Chem.*, 2022, **65**, 190–196.

139 H. Veldhuizen, S. A. Butt, A. Van Leuken, B. Van Der Linden, W. Rook, S. Van Der Zwaag and M. A. Van Der Veen, *ACS Appl. Mater. Interfaces*, 2023, **15**, 29186–29194.

140 A. K. Sekizkardes, P. Wang, J. Hoffman, S. Budhathoki and D. Hopkinson, *Mater. Adv.*, 2022, **3**, 6668–6686.

141 H. L. Nguyen, C. Gropp, N. Hanikel, A. Möckel, A. Lund and O. M. Yaghi, *ACS Cent. Sci.*, 2022, **8**, 926–932.

142 L. Chen, W. Han, X. Yan, J. Zhang, Y. Jiang and Z. Gu, *ChemSusChem*, 2022, **15**, 202201824.

143 C. Sun, Y. Zhu, P. Shao, L. Chen, X. Huang, S. Zhao, D. Ma, X. Jing, B. Wang and X. Feng, *Angew. Chem., Int. Ed.*, 2023, **62**, e2022171.

144 L. Grunenberg, G. Savasci, S. T. Emmerling, F. Heck, S. Bette, A. C. Bergesch, C. Ochsenfeld and B. V Lotsch, *J. Am. Chem. Soc.*, 2023, **145**, 13241–13248.

145 Y. Liu, W. K. Han, W. Chi, J. X. Fu, Y. Mao, X. Yan, J. X. Shao, Y. Jiang and Z. G. Gu, *Appl. Catal., B*, 2023, **338**, 123074.

146 P. W. Fritz and A. Coskun, *ACS Cent. Sci.*, 2022, **8**, 871–873.

147 X. Yuan, N. Wu, Z. Guo and H. Zhan, *Microporous Mesoporous Mater.*, 2023, **355**, 112573.

148 S. Maiti, J. K. Sharma, J. Ling, D. Tietje-Mckinney, M. P. Heaney, T. Runčevski, M. A. Addicoat, F. D'Souza, P. J. Milner and A. Das, *Macromol. Rapid Commun.*, 2023, **44**, 2200751.

149 C. Wang, S. Jiang, W. Ma, Z. Liu, L. Liu, Y. Zou, B. Xu and W. Tian, *Molecules*, 2023, **28**, 449.

150 Q. Liao, W. Xu, X. Huang, C. Ke, Q. Zhang, K. Xi and J. Xie, *Sci. China: Chem.*, 2020, **63**, 707–714.

151 Y. Yang, W. Zhao, H. Niu and Y. Cai, *ACS Appl. Mater. Interfaces*, 2021, **13**, 42035–42043.

152 C. Gao, X. Zhang, M. Zhang, X. Wu, R. Chen, C. Zhang, C. Sun, Y. Du, Q.-H. Xu and B. Hu, *ACS Appl. Energy Mater.*, 2023, **6**, 427–9433.

153 L. Zhang, C. Sun, S.-J. Xiao, Q.-G. Tan, G.-P. Yang, J.-Q. Fan, Y.-T. Luo, R.-P. Liang and J.-D. Qiu, *ACS Appl. Nano Mater.*, 2023, **6**, 17083–17091.

154 C. Arqueros, F. Zamora and C. Montoro, *Nanomaterials*, 2021, **11**, 1–31.

155 Z. Xia, Y. Zhao and S. B. Darling, *Adv. Mater. Interfaces*, 2021, **8**, 1–17.

156 A. K. Mohammed and D. Shetty, *Environ. Sci.: Water Res. Technol.*, 2021, **7**, 1895–1927.

157 S. Kim, H. Wang and Y. M. Lee, *Angew. Chem., Int. Ed.*, 2019, **58**, 17512–17527.

158 J. Li, Y. Li, Y. Lu, Y. Wang, Y. Guo and W. Shi, *Biomimetics*, 2023, **8**, 35.

159 L. Feng, C. Qian and Y. Zhao, *ACS Mater. Lett.*, 2020, **2**, 1074–1092.

160 J. Ma, T. Shu, Y. Sun, X. Zhou, C. Ren, L. Su and X. Zhang, *Small*, 2022, **18**, 1–30.

161 A. Mal, H. Ding, M. Li, W. Li and C. Wang, *ACS Appl. Nano Mater.*, 2022, **5**, 13972–13984.

162 F. Mohajer, G. Mohammadi Ziarani, A. Badiei, S. Iravani and R. S. Varma, *RSC Adv.*, 2023, **13**, 8136–8152.

163 P. Mohan, B. Sasikumar, S. A. G. Krishnan and G. Arthanareeswaran, *J. Taiwan Inst. Chem. Eng.*, 2023, 105067.

164 H. H. Zhang, C. Gu, M. S. Yao and S. Kitagawa, *Adv. Energy Mater.*, 2022, **12**, 2100321.

165 J. Tang, C. Su and Z. Shao, *Small Methods*, 2021, **5**, 1–29.

166 Q. Wang, D. Wang, Q. Liao, C. Ke, Y. Zhang, Q. Han, Y. Zhang, D. Jiang and K. Xi, *J. Colloid Interface Sci.*, 2022, **612**, 608–616.

167 Q. Wang, K. Tang, Q. Liao, Y. Xu, H. Xu, Y. Wang, P. Wang, Z. Meng and K. Xi, *Adv. Funct. Mater.*, 2023, **33**, 2211356.

168 Y. Xiong, Q. Liao, Z. Huang, X. Huang, C. Ke, H. Zhu, C. Dong, H. Wang, K. Xi, P. Zhan, F. Xu and Y. Lu, *Adv. Mater.*, 2020, **32**, 1907242.

169 X. Wu, X. Zhang, Y. Li, B. Wang, Y. Li and L. Chen, *J. Mater. Sci.*, 2021, **56**, 2717–2724.

170 J. Hu, S. K. Gupta, J. Ozdemir and H. Beyzavi, *ACS Appl. Nano Mater.*, 2020, **3**, 6239–6269.

171 H. L. Nguyen, *Chem. Sci.*, 2021, **12**, 8632–8647.

172 B. Gui, J. Xin, Y. Cheng, Y. Zhang, G. Lin, P. Chen, J.-X. Ma, X. Zhou, J. Sun and C. Wang, *J. Am. Chem. Soc.*, 2023, **145**, 11276–11281.

173 Y. Liu, J. Li, J. Lv, Z. Wang, J. Suo, J. Ren, J. Liu, D. Liu, Y. Wang, V. Valtchev, S. Qiu, D. Zhang and Q. Fang, *J. Am. Chem. Soc.*, 2023, **145**, 9679–9685.

174 X. Liu, C. Wang, J. Li, Z. Zhang, A. M. Al-enizi, A. Nafady, F. Shui, Z. You, B. Li, Y. Wen and S. Ma, *Nat. Commun*, 2023, **14**, 7022.

175 P. Martinez-Bulit, A. Sorrenti, D. R. S. Miguel, M. Mattera, Y. Belce, Y. Xia, S. Ma, M.-H. Huang, S. Pané and J. Puigmartí-Luis, *Chem. Engg. J.*, 2022, **435**, 135117.

176 W. Zhang, L. Chen, S. Dai, C. Zhao, C. Ma, L. Wei, M. Zhu, S. Y. Chong, H. Yang, L. Liu, Y. Bai, M. Yu, Y. Xu, X. W. Zhu, Q. Zhu, S. An, R. S. Sprick, M. A. Little, X. Wu, S. Jiang, Y. Wu, Y. B. Zhang, H. Tian, W. H. Zhu and A. I. Cooper, *Nature*, 2022, **604**, 72–79.

26370 | *J. Mater. Chem. A*, 2023, **11**, 26340–26370

This journal is © The Royal Society of Chemistry 2023